Seitz, Iris; Shaukat, Ahmed; Nurmi, Kurt; Ijäs, Heini; Hirvonen, Jouni; Santos, Hélder A.; Kostiainen, Mauri A.; Linko, Veikko

Prospective Cancer Therapies Using Stimuli-Responsive DNA Nanostructures

Published in:
Macromolecular Bioscience

DOI:
10.1002/mabi.202100272

Published: 01/12/2021

Document Version
Peer-reviewed accepted author manuscript, also known as Final accepted manuscript or Post-print

Prospective Cancer Therapies Using Stimuli-Responsive DNA Nanostructures

Iris Seitz,[1] Ahmed Shaukat,[1] Kurt Nurmi,[2] Heini Ijäs,[1,3] Jouni Hirvonen,[4] Hélder A. Santos,[4,5] Mauri A. Kostiainen,[,1,6] and Veikko Linko,*[,1,6]*

[1] Biohybrid Materials, Department of Bioproducts and Biosystems, Aalto University, P.O. Box 16100, 00076 Aalto, Finland

[2] Drug Research Program, Division of Pharmaceutical Biosciences, Faculty of Pharmacy, University of Helsinki, 00014 Finland

[3] Nanoscience Center, Department of Biological and Environmental Science, University of Jyväskylä, P.O. Box 35, 40014 Jyväskylä, Finland

[4] Drug Research Program, Division of Pharmaceutical Chemistry and Technology, Faculty of Pharmacy, University of Helsinki, 00014 Finland

[5] Helsinki Institute of Life Science (HiLIFE), University of Helsinki, 00014 Finland

[6] HYBER Centre, Department of Applied Physics, Aalto University, P.O. Box 15100, 00076 Aalto, Finland

KEYWORDS: DNA nanotechnology, DNA origami, chemotherapeutics, stimuli-based drug delivery,

aptamers, immunostimulation

ABSTRACT

Nanostructures based on DNA self-assembly present an innovative way to address the increasing needs for target-specific delivery of therapeutic molecules. Currently, most of the chemotherapeutics being used in clinical practice have undesired and exceedingly high off-target toxicity. This is a challenge in particular for small molecules, and hence, developing robust and effective methods to lower these side effects and enhance the antitumor activity is of paramount importance. Prospectively, these issues could be tackled with the help of DNA nanotechnology, which provides a route for fabrication of custom, biocompatible, and multimodal structures, which can, to some extent, resist nuclease degradation and survive in cellular environment. Similar to widely employed liposomal products, the DNA nanostructures (DNs) are loaded with selected drugs, and then by employing a specific stimulus, the payload can be released at its target region. In this review, we explore several strategies and triggers to achieve targeted delivery of DNs. Notably, we explain different modalities through which DNs can interact with their respective targets as well as how structural changes triggered by external stimuli can be used to achieve the display or release of the cargo. Furthermore, we highlight the prospects and challenges of this technology.

1. Introduction

Nanotechnology provides highly sophisticated and appealing features for medical science, in particular to cancer therapeutics. There exist FDA-approved nanomedicine therapies which are currently being used in clinical practice with the aim to improve the outcomes of treatments often associated with unsolicited damage to healthy cells [1]. The rather complex and still understudied physiology and heterogeneity of tumors make every prevalent therapy method challenging, but nanotherapies could provide specific advantages over the common regimens in multiple ways [2–5]. One of the advantages of using nanosized therapeutics is that the delivered nano-objects, such as liposomes and other nanoparticles, may concentrate in the tumor region. This may happen through the enhanced permeability and retention (EPR) effect [6,7], however, EPR stands as a rather controversial paradigm. EPR has been sometimes taken as a generalized principle associated with all types of cancer without considering tumor heterogeneity [8]. Therefore, further investigation is necessary to elucidate the mechanism of nanoparticle accumulation in the tumor microenvironment. Apart from higher efficacy and the improved pharmaceutical characteristics of the chemotherapeutic drugs, smaller doses and acquisition of higher specificity may reduce the dose-dependent toxicity in the peripheral area [9–11]. A number of stimuli-based therapies using different drug delivery systems have been proposed and demonstrated, noticeably lipids [12], carbon nanotubes [13,14], protein-based materials, *e.g.*, protein cages [15], virus-like particles [15,16], polymers [17], DNA assemblies [18] and silica-based materials [19,20].

From the abovementioned systems, the design of DNA assemblies is based on structural DNA nanotechnology, pioneered by Nadrian Seeman in the early 1980s [21]. The foundation of DNA nanotechnology lies in the concept of constructing polyhedral objects from DNA using programmable Watson–Crick base pairing. Recently, DNA nanotechnology has paved a way for larger and more complex two- and three-dimensional structures such as DNA origami [22]. The robust and rather straightforward DNA origami design technique is based on folding a long single-stranded DNA scaffold (usually derived from the M13 bacteriophage) into a desired shape with virtually any geometry by using short synthetic DNA strands, *i.e.*, the staple strands that are complementary to multiple segments of the scaffold [23,24].

This review focuses on stimuli-responsive cancer therapies that are based on various DNA nanoassemblies. First, we highlight the properties of DNA-based nano-objects, describe the advantages and limitations of DNA nanostructures (DNs) and the relevance of their combination with a variety of drugs utilized for cancer therapy. It is followed by the introduction of possible cargo molecules and the cellular uptake properties and intracellular fates of the structures. Finally, a thorough overview of the most relevant therapies is presented, organized by the method of eliciting the response, such as design- or environment-based strategies **Figure 1**.

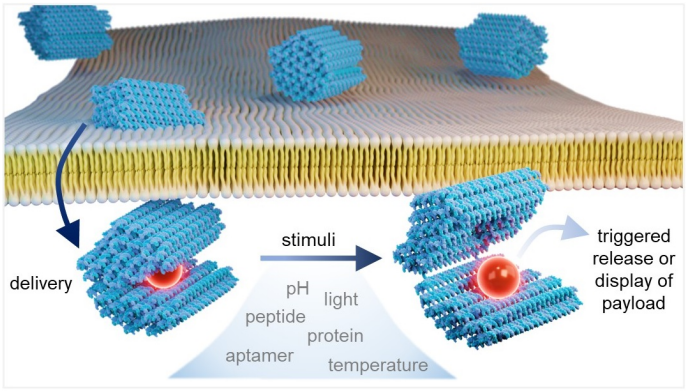

Figure 1. Schematic representation of one type of stimuli-based DNA nanostructures (blue) reviewed in this article. Bottom panel summarizes the classes of stimuli that can be used in DNA-based cancer therapy.

2. Properties of DNs in Drug Delivery

There exists a great diversity of DNs developed for drug delivery and the treatment of different cancer types. An overview of the properties of selected systems is given in **Table 1**. The variety of DN geometries with sizes ranging from a few nanometers up to micrometers reflects the versatility of DNA as a material to build from bottom-up. The performance of DN drug delivery systems in combination with several anticancer drugs and stimuli-responsive sequences or targeting agents for increased specificity has been studied in various cell lines. Further discussion on the anticancer drugs that have been successfully combined with DNs, as well as on the cellular uptake of DNs, is presented in subsections 2.2 and 2.3.

Table 1. List of selected functionalized DNA nanosystems used in the recent literature with their physical properties, type of cargo and cell viability

DN type	Size / ζ-potential	Cargo	Trigger/ Target	Cell line	Efficiency (Cell viability)	Ref.
Triplex DNA nanoswitch on Au-NP	26 nm / N.A.	DOX/cisplatin, antisense DNA	pH	HeLa and L02	~10 % for HeLa and ~30 % for L02	[25]
DNA Nanogel	115.0 nm / −44.8 mV	DOX	pH and GSH-triggered	A549, BEAS-2B, H1299 and LL2 cells	~0% (for all tested cell lines)	[26]
DNA microcapsule	~3200 nm / N.A.	DOX	Light and pH	MDA-MB-231	75%	[27]
DNA i-motif complex	126.0 nm / +16.1 mV	DOX	pH	HeLa and A549	20 % in HeLa and 38.2 % in A549	[28]
octahedral DNA nanocage	N.A / N.A.	DOX	Folate receptors	HeLa and A431	16.7 % in HeLa and no effect in A431	[29]
DNA modified Au-NP	144 nm / N.A.	DOX	AS1411/pH	HeLa	~20 %	[30]
DNA tetrahedron	17.27 nm / -9.56 mV	DOX	Neuropilin-1 binding peptide	U87MG	~30 %	[31]
Polypod-like DN	N.A / N.A.	CpG1668	CpG1668 (TLR9 target)	RAW 264.7 and mice	N.A	[32]
DNA microcapsule	2500 nm / N.A.	CpG	Endocytosis (TLR9)	RAW 264.7	N.A	[33]
DNA origami-gold nanorod	Triangle: 120 nm Tubular: 380 nm / N.A.	Au nanorod	Endocytosis	MCF7 and mice with MCF7 xenograft	~15 %	[34]
Hexapod-like DN	~50 nm / N.A.	A151 CpG	N.A	RAW264.7	N.A	[35]
DNA tetrahedron	22 nm / N.A.	DOX	Cetuximab	NIH 3T3 and MDA-MB-468	~40 % for NIH 3T3 and ~15 % for MDA-MB-468	[36]

N.A. = not available, DOX = doxorubicin

2.1. Advantages and Limitations of Employing DNs

Nanoparticle-based drug systems can be categorized as inorganic, organic and hybrid materials, with each of them showcasing their specific advantages and limitations. Inorganic nanoparticles, such as

silica and metal nanoparticles, can be easily synthesised, while liposomes and polymeric micelles, belonging to the group of organic nanoparticles, can be loaded with either hydrophilic or hydrophobic drugs [37]. However, a certain degree of toxicity is reported for these materials [38]. As an example, due to the hydrophobic nature of carbon nanotubes, not only the solubility in aqueous media is limited, but also toxic aggregates might be formed, for which reason reducing the toxicity is a central focus in the development of these materials [39]. DNs on the contrary are well-suited for the development of robust drug delivery systems [40]. As a type of organic, bio-based nanoparticle, DNs exhibit intrinsic biocompatibility that enables their internalization by mammalian cells, tuneable immunogenicity, and reduced or low toxicity [41]. Both organic and inorganic nanomaterials can be surface-modified or equipped with an abundance of functional groups in a rather straightforward manner [38]. Nevertheless, the key advantages of DNA-based particles are their high programmability and superior addressability. In other words, their precise shape, the placement and number of functional units, and their predefined functions can all be controlled [42]. Therefore, they have been extensively studied as potential bioimaging and diagnostic tools and for the applications combining both diagnostics and therapeutics, *i.e.*, theranostics.

In general, chemotherapy has always been one of the preferred choices of treatment for cancer. However, the available treatments possess growing limitations because of the development of multiple-drug resistance and the characteristic toxicity against healthy tissues. Improved therapy results can be obtained by decreasing the minimum effective dose through higher drug potency, or by selectively delivering the drug resulting in a higher dose for the desired cells/tissue [43]. DNs have multiple avenues and capacity to load cargo materials, which leads to higher internalization [42] and the precise spatial control over the selected payload [44]. Additionally, the drug may be protected from degradation by DNA which prolongs the circulation time at the tumor site. Furthermore, delivering chemotherapeutic drugs with DN carriers has also been presented as an opportunity to treat drug-resistant tumors [45].

Stimuli-responsive DN drug carriers can further enable the selective delivery of drugs to the target cells or the release of the drugs at the target site upon an aimed response to a specific trigger. Selectivity can be, for example, achieved by targeting a distinctive overexpression in tumor cells, preferably on the cell surface, or by a system's sensitivity to environmental changes. By equipping DNs with selected functional groups, the carriers may respond to various environmental stimuli, such as light or change in pH or temperature, or elicit an internal targeting function towards a particular cell type. As a result, non-specific interactions with healthy adjacent tissue can be prevented, minimizing the toxicity of the drug-loaded DNs.

The limitations of the DNs must, however, be carefully considered and they may vary in a structure-dependent manner. The stability of DNs in cellular environments is crucial in a plethora of applications, such as in drug delivery or sensing [46–48], as rapid disintegration might result in early release of the cargo [46]. In the literature, Mg^{2+} concentration and nuclease digestion (thoroughly reviewed by Chandrasekaran [49]) are described as important stability parameters. Commonly, folding of DNA origami structures requires a relatively high concentration of Mg^{2+} ions (millimolar range) for electrostatic repulsion screening, but these kind of concentrations of free Mg^{2+} are not necessarily present *in vitro* and *in vivo* [50]. The sensitivity to cation depletion and to the subsequent degradation has been found to be structure- [46,50] and buffer-dependent [50].

Compared to single-stranded DNA (ssDNA) or dsDNA, DNs have been found to be more stable in physiological environments [47,51]. The higher stability towards nuclease digestion is suggested to arise from steric hindrance, that is, some (embedded) DN domains may not be accessible to enzymes [51]. This might be further tuned by structural design, for example by the strategic introduction of crossovers at exposed sites of the structure. The DNA crossover is defined as a junction at which one DNA strand winds along another helix-strand thereby joining the two parallel helices in the process [52]. For example, structures with paranemic crossover (PX) motifs, which have crossover spacings of 5 to 6 bp, have shown increased stability compared to the widely used double-crossover (DX) motif [53]. Intriguingly,

also the chirality of DNA plays a role in stability as D-DNA mirroring L-DNA tetrahedrons have been reported to exhibit enhanced serum stability [54].

In general, multilayer objects might be favorable for the transport of encapsulated cargo since the closely packed double-helical domains may serve as a shield against degradation [55]. Apart from the structural design, the nano-objects can be protected using a cornucopia of chemical modifications, including single-end modifications with hexaethylene glycol or hexane diol [56], or bio-inspired coatings with e.g., proteins [57] or cationic polymers [58–60]. The possible mechanisms and the related techniques regarding chemical modifications and endonuclease degradation protection strategies have been extensively reviewed elsewhere [61–66]. Despite the prospects of chemical modification, the purification of the nanostructures after conjugation/complexation with functional groups, for instance targeting groups, may turn out rather challenging. Nevertheless, it is important in order to minimize the interference of unbound functional groups. Thereby, denaturation of both functional groups and the DN should be avoided [67].

Concerning the biological stability of DNs, a particular attention should be paid to *in vitro* testing where fetal bovine serum (FBS) is often used as a supplement in cell culture media. The level of nuclease activity in FBS is known to vary which can lead to non-reproducible results [46] and underestimation of the stability of DNs *in vivo*. Nuclease activity in FBS-supplemented culture media, which contains typically 10–20 % FBS, was found to correspond to a DNase I activity between 256 and 1024 U/L [46]. In comparison, DNase I activity in blood plasma was reported to be 360 ± 200 U/L [68]. In order to guarantee reproducible results, the nuclease activity in FBS can be reduced for instance by nuclease inhibitors or heat inactivation [46].

Furthermore, the cost-effectiveness and the scalability of production of DNs are important factors that need to be taken into account when modelling the possible regimen. Currently, DNA origami is estimated to cost 241 €/mg based on commercially available materials [69]. By using biotechnological mass production, a price of 0.18 €/mg of folded DNA origami could be achieved [70]. Translating *in*

vivo results of animal studies to a human (~75 kg), <10 €/dose for DNA has been estimated [63]. Coleridge and Dunn [69] have assessed the cost-effectiveness of DNA nanostructure-based therapies using the quality-adjusted life year (QALY) concept, which combines the quality of life and the additional years of life gained by a new treatment. Apart from the DNA nanostructure production costs of 0.18€/mg, they have considered additional parameters such as the mass of the loaded drug and its cost, R&D costs and the time to recoup the costs. They designed a mathematical expression for two different scenarios, in which either the quantity of drug was considered constant while increasing the QALY, or a constant number of QALY was assumed while decreasing the mass of the drug. For the first scenario, slightly more than half (51.3%) of their parameter set yielded cost-effective therapies for providing an increase of maximum 0.25 QALYs given that one QALY is worth 36145 €. In the second scenario, by reducing the amount of drug by 80 % resulting in a net cost saving, 55.3 % of the parameter sets would result in a nanostructure-based therapy which is more cost-effective than using the drug alone. These results suggest the high potential of commercialization of DN-based therapies under the condition of large-scale and low-cost DNA nanostructure manufacturing [69].

2.2. Cargo Molecules for Drug Delivery

One of the most widely used drugs in cancer treatment is the anthracylic molecule doxorubicin (DOX). It has been ascribed to different mechanisms of actions, but the cytotoxicity is mainly achieved by the interaction of the drug with the DNA-topoisomerase II complex or through the production of free radicals [71]. DNs in combination with DOX have been suggested as a treatment option for drug-resistant tumors. For instance, 2D triangular and 3D tubular origami intercalated with DOX could outperform free DOX in terms of cellular internalization and tumor-killing activity in DOX-resistant adenocarcinoma cancer cells (MCF-7) [45]. It has been long known that DOX has the ability to intercalate into DNA [72,73], and multiple studies have observed its release patterns in acidic environments [29,31,74–78]. The affinity of the intercalator is considerably affected by the design and structure of DNs [79–81], for tile-based DNs it was for instance shown that the inner helices are less exposed to intercalation due to the proximity of the helices causing steric or electrostatic effects [82]. However, it is important to note

that the results obtained with DNs and DOX have left a plenty of room for speculation of the real chemotherapeutic potential of such structures and complexes, as in many studies the DOX loading capacity has been heavily overestimated [79].

In a recent study, a DNA nanotube was combined with the DNA-intercalator daunorubicin (a close relative to DOX) and the complex was tested in HL-60/ADR multidrug-resistant leukaemia cells [83]. After one hour of incubation, the nanotubes were accumulated inside the lysosomes where the cargo was then released. The mechanism for the release of daunorubicin was suggested to be mediated by the degradation of the nanotubes, thus inducing cell death. The authors suggested, furthermore, that DNs can dodge the efflux-pump-mediated drug resistance in leukaemia cells, and hence, can elicit a high activity at clinically relevant levels [83].

DNs have also been combined with the platinum-based drugs cisplatin and 56MESS [84–86]. The effectiveness of cisplatin compared to its Pt(IV) prodrug which was covalently linked to three differently shaped DNs constructed with the brick method was observed in cisplatin-resistant cancer cells (A549cisR) and in non-resistant lung cancer cells (A549) [87]. The results showed that the DNs could remarkably enhance the cellular internalization of platinum drugs, and thus, increase the anticancer activity for these resistant cell lines. Furthermore, the *in vivo* results obtained from A549 xenograft-bearing nude mice showed effective suppression of the tumor growth in both regular and cisplatin-resistant tumor models [87].

It has now been established in clinical practice that there is an acute problem of cell resistance to 5-fluorouracil (5-FU), which can be attributed to various mechanisms [88] including an increased rate of deoxythymidine monophosphate biosynthesis [89] and increased 5-FU catabolism aided by dihydropyrimidine dehydrogenase (DPD) [90]. Thus, it is significant that methods to circumvent such resistance are carefully examined. It was observed that by combining 5-FU and 5-fluoro-2'-deoxyuridine decamer (FdU_{10}) with tetrahedral DNs (TDNs) with cholesterol acting as a promoter of cellular uptake, higher *in vitro* cytotoxic and anti-proliferative effects in HCC2998 and HTB-38 cell

lines were obtained [91]. These cell lines are known for different selectivity against conventional drugs, 5-FU and FdU_{10} and hence employing TDNs provides the optimum concentration required to elicit a strong response.

Furthermore, the less studied method is to take advantage of groove-binding drugs. Paclitaxel (PTX) is one example of a groove-binding drug, with a preference for AT rich sequences [92,93]. A study with PTX-loaded TDNs was conducted in non-small cell lung cancer (NSCLC) cells (A549) and in a PTX-resistant cell line [94]. The combination of PTX/TDNs resulted in high cytotoxicity on both the resistant and the non-resistant cancer cell lines. It was also found that the cause of resistance in tumors was associated with downregulation of multi-drug resistance gene 1 and P-glycoprotein (P-gp). The authors suggested that TDNs may serve as a P-gp inhibitor to circumvent the resistance, however, the exact mechanism still needs to be further explored [94]. Further investigations on loading DNA origami structures with groove-binding drugs have been carried out using methylene blue (MB), which can act either as a minor groove binder or as an intercalator depending on the salt concentration. The binding affinity of MB was found to be dependent on the superstructure of the employed DNA origami [95].

2.3. Uptake and Internalization of DNs

DN internalization is highly dependent on multiple factors, such as their physical characteristics (*i.e.*, size, mass, shape and density) [96,97] and cell line type [98] used in the experiments. The cellular intake pathway could be endocytic [78,83,99] or non-endocytic [61]. Fluorescence-based techniques, such as Förster resonance energy transfer (FRET) and confocal microscopy can be employed to track and quantify the uptake of the DNs inside the cell [100]. For tile-based structures, internalization by caveolae-mediated endocytosis has been observed [101,102], whereas the uptake of DNA origami can be mediated by scavenger receptors [98,103].

The fate of the DNs after crossing the cell membrane (extensively reviewed elsewhere [104]) usually involves the endolysosomal pathway. For example, DNA octahedral nanocages were found to

accumulate in the lysosomes of COS fibroblasts [105]. TDNs were also localized in lysosomes when transfected into HeLa cells. Their uptake was found to be size- and cell-dependent; the smaller the size, the faster the entry with a preference for cancer cells [106]. In another study, DNA origami nanotubes were tracked using cyanine in MCF-7 cells [107]. The nanotubes could be detected via fluorescence in lysosomes after 12 h of incubation (after the cells were replenished with fresh media, *i.e.*, without the nanotubes). Continuous reduction of intracellular fluorescence was observed over the course of 60 h, suggesting a breakdown of the nanotubes. This controlled degradation could be used to formulate a sustained release of a potential co-delivered drug [107].

3. Environment-Based Stimuli-Responsive Strategies

DNs have been found to release their cargo due to structural change or disintegration of the transport vehicle upon environmental stimuli. Thereby, the external cue can be used as a trigger to release chemotherapeutics from a DNA vehicle in a controlled manner. The three most prominent and also promising stimuli for this purpose – light, and the change of internal conditions in pH, and temperature – are reviewed in the following subsections.

3.1. pH-Based Stimuli

pH-activated DNs present a novel approach for a stimuli-responsive design to overcome nonspecific interactions and to circumvent multidrug resistance. So far, mainly the acidic pH-value in the lysosomes (4.5–5.5) has been exploited together with other lysosomal degradation mechanisms in order to trigger the release of intercalated or entrapped chemotherapeutics [77,78,108,109]. Reversed pH-values in the cancer cell microenvironment, however, provide an attractive approach for stimuli-based targeting and selective delivery of chemotherapeutics for a temporal and spatial release.

The extracellular pH value of tumors tends to be decreased to ~6.8–7.0 compared to the usual ~7.4 [110] which is thought to occur due to the secretion of acidic metabolites, like lactic acid [111,112].

Simultaneously, cancer cells maintain a high intracellular pH value, ~7.3–7.6 compared to ~7.2 in healthy cells, which is not only necessary for cell proliferation and promotion of metastasis initiation, but also for decreased apoptosis. Furthermore, the altered pH properties stimulate cell migration and invasion [110].

Most designs presented in the literature would prefer additional targeting extensions, such as pH-responsive aptamer sequences that are discussed later in subsection 4.2 [110] or pH-based nanocomposites releasing multiple drugs at the cancer site [113]. Here, the current trends in pH-responsive DN designs and their working principles are reviewed.

The most commonly employed functional units in pH-triggered DNs in cancer therapeutics are i-motif and DNA triplex structures. An i-motif structure is a pH-responsive cytosine (C)-rich oligonucleotide, which forms an anti-parallel tetramer structure (quadruplex) through C-CH^+ pairing at low pH [28]. In DNA triplexes, a third strand binds to the major groove of a duplex by Hoogsteen or reverse Hoogsteen hydrogen bonds [114].

The i-motif structures have been used as pH-responsive lock-mechanisms in combination with nanoparticles, or as "hinges" in TDNs or DNA origami [27,30]. Sun *et al.* [30] used AuNP as the deposition substrate for short DNA strands, which were elongated by terminal deoxynucleotidyl transferase to increase the thickness of the DNA layer. The DNA strands were designed to be capable of forming an i-motif structure to subsequently release the cargo molecule DOX. Additionally, they were hybridized to the AS1411 aptamer as a targeting moiety which resulted in a reduced cell viability in nucleolin-overexpressing HeLa cells [30]. A study conducted by Huang *et al.* [27] depicts a different approach by using the i-motif structure as a pH-responsive bridging agent in a multi-layered DNA microcapsule. The capsule was composed of six layers of oligonucleotides which were connected by i-motif forming sequences (**Figure 2**a). These oligonucleotides were deposited onto a positively charged $CaCO_3$ core which contained CdSe/ZnS quantum dots and DOX as model drugs. The $CaCO_3$ core was subsequently removed by etching, resulting in free cargo molecules. To avoid leakage of DOX, it was covalently

bound to dextran *via* boronic esters. This ester bond can be cleaved at a low pH at which also the microcapsule is expected to disassemble. An increase in fluorescence indicates the decomposition of the oligonucleotide shell and subsequently the release of the quantum dots at pH 5. Even though the study did not describe conclusively the effect of the microdevice on cancer cells (MDA-MB-231, MCF-10A), the design offers an interesting perspective of applying such systems in cancer therapeutics [27]. These studies demonstrate that an i-motif structure can be readily incorporated into larger DNs, even though it is challenging to engineer the i-motif structure that is operational over a wide pH-range [115].

Chen *et al*. [25] demonstrated a DN design in which the DNA triplex was attached to a AuNP, and the AuNP was further functionalized by MUC1 aptamer (**Figure 2**b). This design supported the idea of multidrug loading capacity; cisplatin was attached to a therapeutic antisense DNA (asDNA), which in turn was bound to the triplex DNA forming moiety on the AuNP. DOX was also loaded into the structure. HeLa cells implanted subcutaneously into mice were used for *in vivo* studies. A 6-fold decrease upon tumor treatment with the multiloaded DNs was observed (compared to free DOX), suggesting the pH-dependent conformation change of DNA in lysosomes leads to the release of DOX, cisplatin and asDNA. *In vitro* studies in HeLa cells led to a drastic decrease of cell viability and showed that the cisplatin consumes glutathione resulting in an accumulation of reactive oxygen species (ROS), which in return leads to membrane damage and supports the escape of DOX and asDNA from the lysosome to their desired locations, nucleus and cytoplasm, respectively [25].

Ijäs *et al*. [116] presented a DNA origami-based nanocapsule (Error! Reference source not found.c) capable of responding to minutiae changes of the pH of the environment. In the study, DNA triplexes worked as reversible "latches", which could control the nanocapsule conformation (open/close) depending on the pH-value of the surrounding solution. The dynamics of the capsule were monitored by FRET as the halves of the capsule were equipped with a FRET forming dye pair. It was discovered that the nanocapsules could be loaded with gold nanoparticles (AuNP) and horse-radish peroxidase (HRP) enzymes at high pH (pH 8.2) (AuNPs had a loading efficiency of 40–55% (n = 110)) and the

cargo could be encapsulated by closing the capsules at low pH (pH 6.4) [116]. This design showcases a straightforward system that could be used in treatments related to the increased intracellular pH-value of certain cancer cells. Nevertheless, this study did not show *in vitro* or *in vivo* results, which could further prove the functionality of designs with such intricate mechanisms.

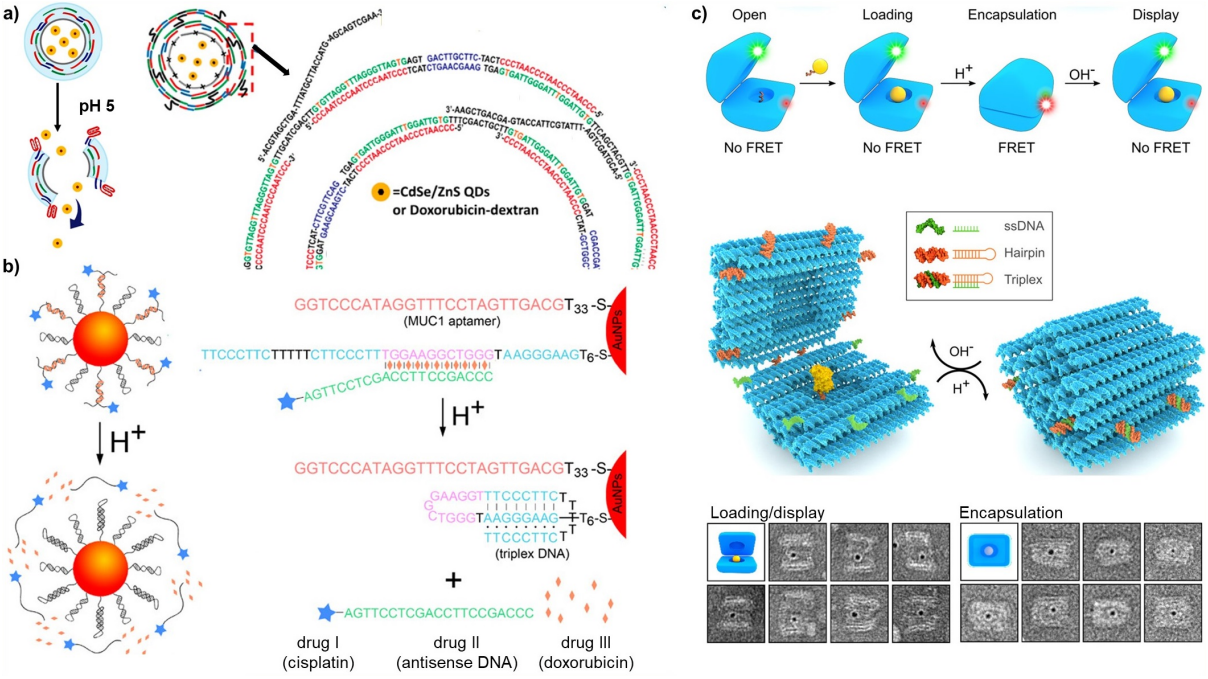

Figure 2. The pH-responsive DN drug delivery systems. a) Release mechanism using i-motif formation of a multi-layered DNA microcapsule (left), design of the layers (blue, red and green strands) and the corresponding bridging unit (black strand) (right). Adapted with permission [27]. Copyright 2016, American Chemical Society. b) Construction of a multidrug nanoparticle system. Release of intercalated DOX (red) and the cisplatin (blue)-modified asDNA from the DNA triplex Au-NP complex. Adapted with permission [25]. Copyright 2019, American Chemical Society. c) A schematic diagram of DNA origami nanocapsule full operational cycle showing loading, encapsulation and display under different pH conditions (top), a schematic diagram of the HRP-loaded DNA nanocapsule using eight programmable pH latches (middle), TEM images of the nanocapsule in loading and encapsulated positions (bottom). Adapted with permission [116]. Copyright 2019, American Chemical Society.

The abovementioned studies exemplify the current applications of DNA triplexes in DNs either as a mechanical latch or as an independent drug carrier. In contrast to the i-motif structure, DNA triplexes offer a higher degree of programmability by varying the relative content of CGC/TAT triplets in the triplex structure, thus enabling controlled fine tuning of the system within a selected pH-range [115]. As a summary, pH-triggered DNs pose themselves as a promising field of study, especially with respect to the treatment of cancer, because of their capability of forming reconfigurable systems in combination with their intrinsic biocompatibility. However, major leaps in DN research must be taken to fully realize a solution translatable into clinical settings.

3.2. Temperature-Based Stimuli

Besides the pH-responsiveness, drug release can also be achieved through local hyperthermia, especially when the delivery vehicles are based on polymeric materials [117]. A great deal of research has been dedicated to thermally responsive polymers, but current knowledge on DNs applying similar principles have yet to be explored in the context of cancer therapeutics. Turek *et al*. [118], for example, attached the thermo-responsive polymer poly(*N*-isopropylacrylamide) (PNIPAM) on each side of a flexible DNA origami region in order to obtain a device working similarly as a tweezer. At temperatures that exceeded the lower critical solution temperature of the polymer, an increase in hydrophobicity was observed, which subsequently resulted in closing of the tweezer [118].

Furthermore, thermo-responsive DNs have been studied by Juul *et al*. [119] and Franch *et al*. [120], who employed octahedral DNA cages for enzyme delivery (HRP). These cages contained a truncated corner, to which four hairpin-forming sequences were attached. These serve as a "gate" and subsequently introduce flexibility into the entire structure (**Figure 3**a). The dimensions of the octahedron were designed to prevent diffusion through the hexagonal side planes confined by the octahedral lattice at low temperature. By increasing the temperature to 37 °C a loosening of the structure was observed allowing the widening of these hexagonal faces to be sufficient enough to encapsulate the HRP molecule. At 4 °C, no encapsulation of free HRP was observed, and in return a trapped HRP could not leave the DNA cage [119]. Further studies revealed the dependency between uptake of HRP and the

number of hairpins (1–4) (**Figure 3**b, left). The highest encapsulation efficiency was obtained for the structure containing 3 hairpins, whereas a clear decrease for ≥1 hairpin was observed (**Figure 3**b, right). In the presence of at least two hairpins, the adjacent surface(s) increased to >23 nm^2 which is sufficient for encapsulation of HRP [120]. These studies showcase the possibilities of a thermally programmable DN design for delivering larger molecules, *e.g.*, enzymes. However, the current temperature range is impracticable for *in vivo* applications. Gareau *et al.*[121] presented a DNA clamp-based architecture, which was inspired by DNA stem-loops and DNA triplexes. The temperature-responsiveness of the structure could be altered by changing the CG content which was facilitated by the addition of stabilizer strands binding to extended stem-loop regions (**Figure 3**c). The multimeric DNA switches (up to 4 strands) showed a steep transition behavior making them suitable for the integration into drug delivery devices [121].

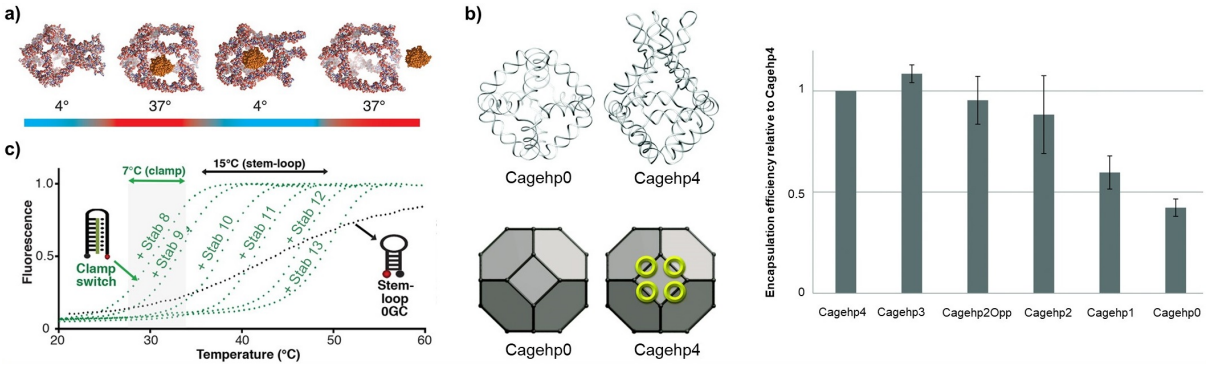

Figure 3. DN drug delivery systems with temperature-responsive behavior. a) Atomistic model of a truncated octahedron cage with 4 hairpins at different temperatures as a schematic representation showing the encapsulation of HRP. Adapted with permission [119]. Copyright 2013, American Chemical Society. b) Schematic representation of the location of hairpins (0 and 4; side and top view) on the truncated octahedral DNA cage (left). Bar chart showing the encapsulation efficiency dependency on the number of hairpins (right). The data was normalized for the cage with 4 hairpins (Cagehp4). Adapted with permission [120]. Copyright 2016, Royal Society of Chemistry. c) Comparison of the fluorescence intensity of an ultrasensitive DNA clamp thermoswitch with stabilizing strands of different length (green) with a stem-loop structure without CG (black). Adapted with permission [121]. Copyright 2016, American Chemical Society.

Additionally, covalent attachment of DNA oligonucleotides of various lengths to mesoporous silica particles resulted in a temperature-dependent release of rhodamine B. Thereby, the DNA served as a "valve" which opened upon a decrease of electrostatic interactions caused by the temperature rise [122].

Despite the novel schemes explored in this section, no conclusive studies yet exist in the field of thermo-programmed DNs in cancer therapeutics. Currently, the lack of comprehensive *in vivo* studies makes it challenging to properly assess the effectiveness of temperature-sensitive DNA nanodesigns. Further research is also required to develop new methods for heating cancerous tissues and subsequently releasing the cargo at the target location.

3.3. Light-Based Stimuli and Other Strategies

Recently, an extensive amount of research has been dedicated to light-based therapies for cancer. The outcomes of these therapies are mediated by the photothermal and photodynamic activities of various optically responsive compounds. These therapy types involve light as a stimulus, which excites the photosensitizing agent and therefore causes it to release heat (photothermal) or cytotoxic ROS (photodynamic). These therapies induce targeted cell death, thus minimizing the damage to adjacent healthy tissues. It was recently shown that DNA-based carrier complexed with photosensitizers DNs may also provide protection from endonuclease degradation, which could then provide a key to prolonged circulation times in the body [123]. AuNPs, in turn, have been at the forefront of creating multifunctional nanoplatforms that allow simultaneous cancer diagnosis and therapy. However, lack of tumor penetration, specificity, modification optimization, and size-irregularities of the AuNPs calls for the use of a nanocarrier that can impart uniform shape and size with precise spatial addressability [124,125].

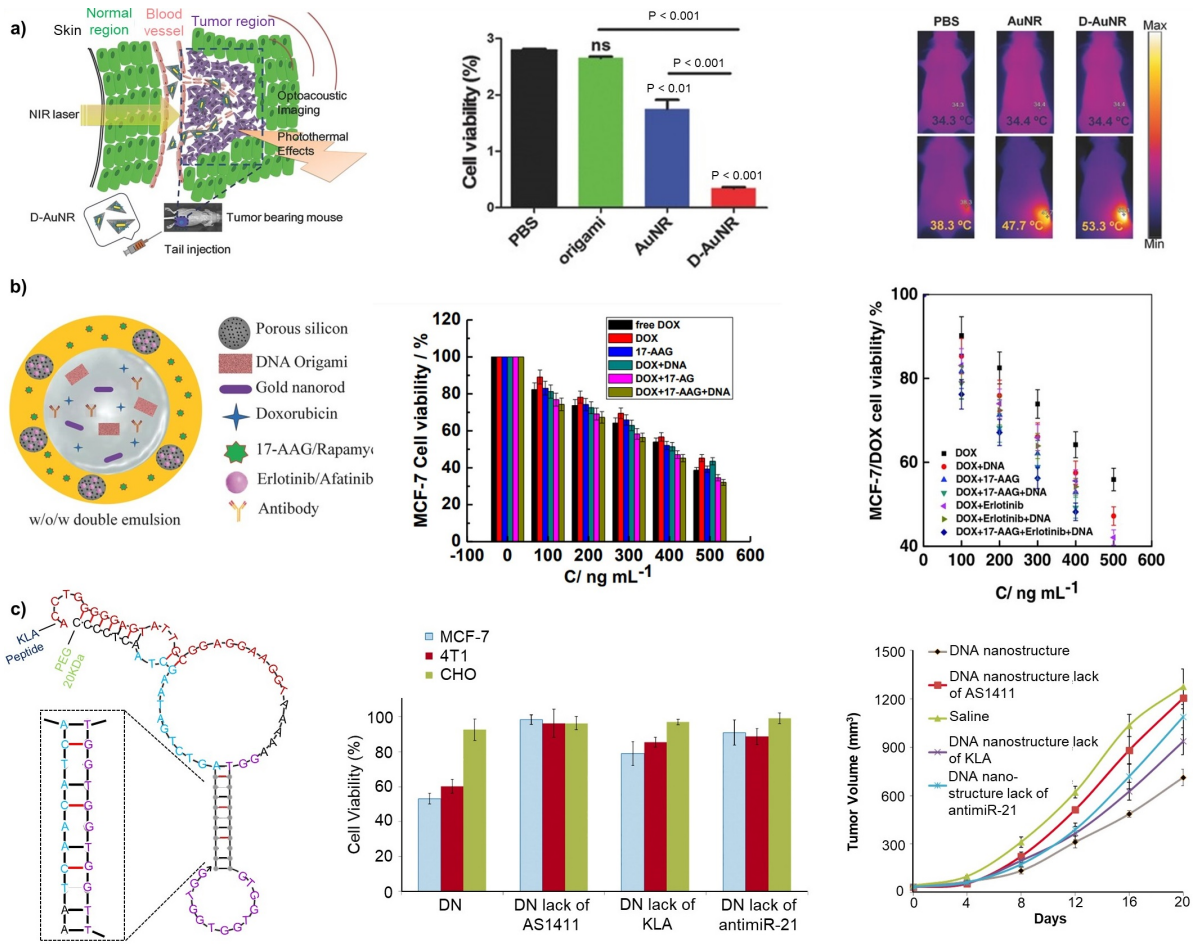

Figure 4. DN drug delivery systems with light as a stimulus. a) DNA-origami-gold-nanorod hybrid (D-AuNR) (left) having better cytotoxicity (middle) in 4T1-fLuc tumor cells and higher photothermal response (right) as compared plain AuNR alone and D-AuNR, with and without NIR laser irradiation (808 nm, 1.5 W cm^{-2}, 3 min) Adapted with permission [126]. Copyright 2016, John Wiley and Sons. b) Water-in-oil-in-water (W/O/W) double emulsion droplet comprised of several hydrophilic (DOX, AuNRs, antibody, DNA origami) and hydrophobic (Psi NPs, 17-AAG/rapamycin) components (left). Cell viability of MCF-7 (middle) and DOX-resistant MCF-7/DOX cells (right) with various combinations of drug load. Adapted with permission [127]. Copyright 2016, John Wiley and Sons. c) Schematic of DN composed of sequences containing ATP (red) and AS1411 (pink) aptamers and antimiR-21 (blue) (left) with cell viability (middle) of DN, DN lack of AS1411, DN lack of KLA peptide and DN lack of antimiR-21 on nontarget (CHO) and target (MCF-7 and 4T1) and (right) the *in vivo* antitumor efficacy of the DN together with other controls against breast tumor allograft on mice administration during 20 days. Adapted with permission [128]. Copyright 2020, Taylor & Francis.

In a recent study, a triangular DNA origami with gold nanorods (AuNR) on its surface (D-AuNR) (**Figure 4**a, left) was created and tested both *in vitro* and *in vivo* for optoacoustic imaging, as well as for photothermal therapy [126]. When AuNRs are irradiated with near-infrared (NIR) rays, they elicit surface plasmon resonance and subsequently release the absorbed energy as heat. The NIR range is well-suited for medical purpose as it has a high tissue penetration without any untoward reactions. The optoacoustic imaging was performed on breast-tumor-xenografted mice in tumors that were grafted to the liver and kidney. Monitoring of the signals of AuNR and D-AuNR as early as 3 h after intravenous injection displayed a similar penetration for D-AuNRs and AuNRs, but the retention of D-AuNRs in the tumor mass was better. To evaluate NIR-responsive photothermal therapeutic efficacy of D-AuNRs, the *in vitro* activity was tested on mouse mammary carcinoma cell line 4T1 (**Figure 4**a, middle). While AuNRs reduced the cell viability to ~63% compared to the control, D–AuNR knocked the cell viability down to ~12.3%, suggesting superior antitumor activity. Moreover, an *in vivo* study on mice bearing mammary carcinoma was conducted by intravenous injections of phosphate buffered saline (PBS), AuNR and D-AuNR. The mice were then irradiated with a NIR laser. The results revealed that the D-AuNR treatment induced the highest temperature rise (from 34.3 to 53.3 °C) in the investigated tissue (**Figure 4**a, right), which can be translated into improved outcome of the tumor therapy [126]. Similar results have been achieved by employing triangular and tubular-shaped DNA origami and MCF-7 cells as well as MCF-7 xenograft tumors [34].

In a different approach, to enhance co-loading and co-delivery of versatile therapeutics, all-in-one biocompatible double emulsion (W/O/W) (**Figure 4**b, left) was formulated from the hydrophilic part containing DNA origami, DOX, AuNRs and fluorescent antibody, and the hydrophobic part comprising erlotinib loaded porous silicon nanoparticles (PSi NPs) and Tanespimycin (17-N-allylamino-17-demethoxygeldanamycin, 17-AAG) (PSi@AuNRs@double emulsion droplets) [127]. Since drugs potentially have different solubilities, co-loading of hydrophilic and hydrophobic anticancer drugs would have a synergistic effect and could improve therapeutic success against multi-drug resistant cancer cells [127]. The release profile of the double emulsion was checked at pH 7.4 (blood) and pH 1.2

(stomach), which suggested that 60–90% of drugs were released within 24 h without initial burst and that the release was faster at pH 1.2. The *in vitro* cytotoxicity assay performed with MCF-7 (**Figure 4**b, middle) and MDA-MB-231 breast cancer cells revealed a synergistic effect of the loaded drugs. It is hypothesised, that the DNA origami within the droplet is involved in enhancing the uptake of DOX into the cells. Also, the DNA origami loaded in PSi@AuNRs@double emulsion droplets produced a stronger cytotoxic effect against DOX-resistant MCF-7/DOX cells (**Figure 4**b, right) than droplets loaded with a single drug. To investigate the photothermal effects of AuNRs within a biocompatible platform, the cells were irradiated using a NIR laser at 750 nm from 5 to 30 min. It was observed that 90% of DOX and AuNRs were released from the carrier within 30 mins of laser irradiation, thus indicating that optimization in laser intensity and exposure as well as concentration of the AuNRs could lead to efficient photothermal therapy [127].

An intriguing method to target cancer cells was recently demonstrated using an ATP-responsive DN delivery system (**Figure 4**c, left) for the co-delivery of KLA peptide and antimiR-21 (antisense of oncogenic microRNA-21) [128]. The cellular adenosine triphosphate (ATP) levels have been found to be between 3 to 10 mM and only 10 nM of ATP is found extracellularly [129,130]. The DN was composed of two aptamer sequences, ATP (red) and AS1411 (pink), as well as the antimiR-21 sequence [128]. AS1411 is an aptamer that binds specifically to nucleolin, an overexpressed protein on the plasma membrane of many kinds of cancer cells [131]. In the presence of high ATP concentrations (6 mM) in the lysosome, the structure was disassembled and antimiR-21 released, which then implemented its activity explicitly in the target cells (**Figure 4**c, middle). It is suggested that the endosomal escape of antimiR-21 was enhanced by the KLA peptide. The activity of antimiR-21 was further proven by *in vivo* mice allograft model (**Figure 4**c, right) in which the tumor growth nearly halved when using the DN compared to saline control over 20 days of intravenous administration [128].

4. Design-Based Strategies

Many studies have used additional molecules to achieve a targeted delivery of the DN. Here, these modifications are referred to as design-based approaches. Simultaneously, a conformational change, *i.e.*, opening of the structure, display/release of drugs, can be triggered depending on the type of the molecular recognition/targeting molecule.

One promising option for targeted delivery is the use of antibodies, which are known for their interaction with antigens with high specificity and affinity [43,132,133]. In addition, aptamers have been introduced as novel techniques with several significant advantages over protein-based delivery systems [134], especially in combination with drug carrier cages based on DNA structures due to their small size. Alternatively, small targeting molecule-drug conjugates and antisense/siRNA delivery have shown promising results for targeted delivery [43].

4.1. Antibodies and Antibody-Derived Proteins

Several mechanisms leading to cell death have been reported for monoclonal antibodies, making them an important, powerful, and widely used tool in cancer therapy by selectively targeting (over)expressed antigens on the tumor tissue surface [43]. High antitumor activity has been reported for monoclonal antibodies targeting the CD20 protein, EGFR or HER2 [135]. By 2020, twenty-three monoclonal antibodies were approved by the FDA for clinical use [135]. The cytotoxicity of monoclonal antibodies can also be enhanced by covalently conjugating them to chemotherapeutic drugs, such as DOX [43].

In addition to serving as drugs themselves, antibodies can also be conjugated to DNs for cancer cell targeting. Setyawati *et al.* [36] conjugated the antibody cetuximab to a DOX-loaded TDN *via* thiol groups. Targeting of the overexpressed EGFR led to a specific and enhanced death of breast cancer cells (MDA-MB-468 cell line) [36]. A modular approach to conjugate antibodies to a DNA origami platform was presented by Rosier *et al.* [136]. There, a variant of protein G (9.6 kDa, protein G has a high binding affinity to Fc region of IgG antibodies [137] was linked to the Fc region of the IgG-type antibody cetuximab by photoconjugation. The N-terminal cysteine of the protein G variant allowed for the

attachment of a 20-nt oligonucleotide which was used as a handle for hybridization to a complementary strand on the DNA origami surface [136]. Using this technique, the binding behavior of an antibody immobilized on differently shaped DNA origami structures to cell surface receptors was investigated [138]. It was shown that the native binding affinity is not affected by the immobilization, but that the binding efficiency is dependent on the size and shape of the origami structure because of the steric hindrance.

Even though promising results have been obtained using antibody-DN conjugates, several challenges regarding the antibody properties have been observed over the years. These include therapeutic resistance [135] and costly production [139,140]. Monoclonal antibodies can be produced in transgenic animals [141] and eukaryotic cell lines [142], or by using phage display [141]. Cell cultures are prone to contamination from bacteria and viruses, which in return requires excessive quality control to ensure the safety of the therapeutic product [142]. Additionally, cross-reactivity, which is desired in animal studies, has to be considered, *i.e.* the antibody is able to detect the antigen even though the species differs from the one where the antigen originates from [143]. The shelf-life of antibodies might be limited by denaturation, but most importantly, access to several cell compartments is prevented due to their large size [139,140]. A decrease in size is achieved by using single-domain antibodies, allowing for high binding affinity even to closely packed receptors [86] and higher penetration into tumor regions distal from the blood vessels [144]. Attachment of an anti-EGFR single-domain antibody (~15 kDa) to a TDN showed directed delivery of the platinum drug 56MESS to EGFR overexpressing cells [86]. The cell viability was drastically decreased and the tumor growth almost fully inhibited [86].

An alternative to antibodies is presented by antibody-mimicking peptides called affibodies. They are considered advantageous because their small size (58 amino acids) allows them to get deeper into the tumor tissue [145]. An affibody with high selectivity against the human epidermal growth factor 2 receptor (HER2) was for instance attached to a TDN (**Figure 5**a, top) in order to treat HER2 overexpressing cells, which are present in different cancer types (*e.g.*, breast, lung, and prostate) [146].

Loading of the TDN with DOX resulted in efficacious and highly selective delivery of the drug to its target and subsequent inhibition of the growth of BT474 cells. A prominent difference compared to DOX was observed at small concentrations. While DOX was able to inhibit 44% after 96 h at a concentration of 320 nM, the nanoparticle loaded with the corresponding amount of DOX achieved 69% inhibition of cell growth (Error! Reference source not found.a, bottom) [146]. Using the same affibody-TDN carrier for cisplatin delivery, a 1.6-fold increase in growth inhibition of BT474 cells was obtained [84]. After 72 h incubation, 82.9% of cell growth was inhibited by 33.3 μM cisplatin, whereas treatment with the nanoparticles resulted in 94.6% inhibition [84]. The effect was more pronounced in cells that highly overexpress HER2 [84,146]. A HER2 affibody was also used by Zhang *et al*. [147] to deliver the antitumor nucleoside analogue 5-fluorodeoxyuridine (FUdR). Polymeric FUdR molecules (consisting of ten FUdRs) were covalently linked to the 5' end of four DNA strands which self-assemble into the TDN. This allows for a precise definition of the drug-load (4 $FUdR_{10}$ drug molecules per TDN). The affibody was subsequently attached to one FUdR-modified DNA strand using N-ε-malemidocaproyl-oxysuccinimide ester (EMCS) to crosslink the C-terminal cysteine with the end of $FUdR_{10}$ (**Figure 5**b, top). Both *in vitro* and *in vivo* tests on the HER2 overexpressing BT474 cell line and on BT474 tumor xenografted mice, respectively, showed an increased accumulation of the nanoparticle in the tumor tissue. The *in vitro* cytotoxicity was found to be dose-dependent, decreasing the cell viability to 18.8% at a concentration of 250 nM in BT474 cells. Treatment with the FUdR TDN without the affibody resulted in 39.8% cell viability (**Figure 5**b, bottom-left). For healthy MCF-10A cells, a higher cell viability was detected for the affibody conjugate in comparison to the drug-loaded TDN, demonstrating the importance of the targeting molecule (**Figure 5**b, bottom-right) [147].

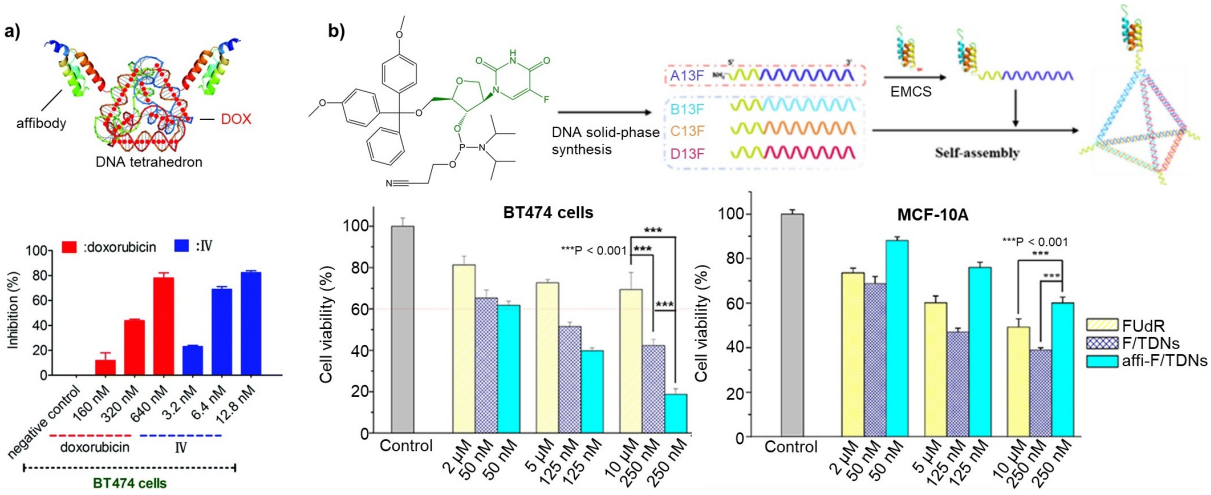

Figure 5. Effects of the use of antibody-derived molecules-DN conjugates on tumor cells. a) DNA tetrahedron–affibody–drug nanoparticle (top) and comparison of cell growth inhibition of BT474 between free DOX and the TDN-affibody nanoparticle (IV) after 96 h (bottom). Adapted with permission [146]. Copyright 2017, Royal Society of Chemistry. b) Preparation and efficiency of affi-F/TDNs. Schematic illustration of preparation of affi-F/TDNs with other three DNA strand using solid-phase synthesis (top). The 5′-NH2 labeled DNA strand, A13F-NH2, was conjugated with affibody *via* EMCS and self-assembled into affi-F/TDNs. Cell viability of HER2 overexpressing BT474 cells (bottom-left) and MCF-10A cells (bottom-right) upon 72 h treatment with FUdR (yellow), FUdR in TDNs (F/TDNs, lila) and FUdR in TDNs with attached HER2-affibody (affi-F/TDNs, cyan). Results are shown as a percentage of the control group. Adapted with permission [147]. Copyright 2020, Dove Medical Press.

4.2. Aptamers

Nucleic acid aptamers are short single-stranded oligonucleotides that are able to bind specific target molecules, and they provide a promising alternative to antibodies and their truncated derivatives. Their binding properties are fully programmable by altering their sequence through the inexpensive synthesis. In general, they are stable at higher temperatures compared to antibodies, and their resistance against nuclease degradation can be increased by chemical modifications [139,140].

Chu *et al*. [148] compared the binding specificity of the aptamer HB5 and the anti-HER2 antibody to HER2-positive breast cancer cells. It was shown that the aptamer exhibited strong binding, but more importantly, the aptamer and the antibody had the same target site for the membrane [148].

The target selection for the corresponding aptamer is performed *in vitro* using the systematic evolution of ligands by exponential enrichment (SELEX) method [149,150]. Thereby, a library of random oligonucleotide sequences is screened for high-affinity binding to the selected target. After separation from unbound aptamers and amplification by polymerase chain reaction (PCR) or reverse transcription PCR (RT-PCR), the process is repeated with the new pool. Variations of this method have been presented, for example, Shangguan *et al*. [151] developed cell-SELEX, in which entire cells can serve as the target. This approach enables the selection of disease cells without knowing the target for aptamer binding and subsequent elucidation of the molecular signature on the cell surface. During the process, the target is in its native configuration, which is advantageous for further clinical application [151]. Additionally, for conduction of the method on adherent cell lines, *e.g*., HeLa cells, adherend cell-SELEX was introduced [152]. Alternatively, a bead-based selection method has been developed, which enables the selection of chemically modified aptamers since these cannot be selected by the traditional SELEX approach due to the incompatibility of polymerase and substrate in the PCR reaction [153].

SELEX and derived methods have resulted in many aptamers with high potential for clinical applications in targeted drug delivery, biosensing and bioimaging. A selection of DNA aptamers is listed in **Table 2**, while other aptamers have been reviewed elsewhere [154,155].

Table 1. List of DNA aptamers including their sequence and the target tissue. The aptamers were generated using cell-SELEX, and the target on the cell surface might therefore still be unknown (marked with N.A.)

Name	Target	Sequence	Application/Cancer type/tissue/Cell line	Ref
XL-33-1	Protein on cell membrane of SW620	CCCATCAATGTTACGACCCGCTAGGG CTGCTGTGCCATCGGGTAA	SW620 cell line, lymph node metastasis of colon cancer	[156]
Cy-apt-20	N.A.	CGACCCGGCACAAACCCAGAACCATA TACAC GATCATTAGTCTCCTGGGCCG	Gastric carcinoma cell line AGS	[157]
MF3	N.A.	AGCAGAGTTCACGACCCGATAAGTGC ATTAGCACGTCCGAGAAAGGCCAGAC GAGGTCACACAGAGTTACATACCAAT CGTCGCAG	Human mammary gland adenocarcinoma (MCF7)	[158]
AGC03	N.A.	ACGCTCGGATGCCACTACAGGGGGGT GGTCCTGAGGGTGGTGTGGTTGGTTT GGTTTCCTCATGGACGTGCTGGTGAC	Gastric cancer line HGC-27	[159]
LXL-1-A	Extracellular protein on MDA-MB-231	GAA TTC AGT CGG ACA GCG AAG TAG TTT TCC TTC TAA CCT AAG AAC CCG CGG CAG TTT AAT GTA GAT GGA CGA A	MDA-MB-231 derived from metastatic site pleural effusion	[160]
Ap52	MAGE-A3$_{111–125}$	ATCCAGAGTGACGCAGCAAGCACTCA ATATTCCCTGGACACGGTGGCTTAGT	Several tumor tissues	[161]
HF3-58	Glycoprotein on A2780T surface	TTGGAGCAGCGTGGAGGATATGCTTT CCGACCGTGTTCGTTTGTTATAACGCT GCTCC	PTX-resistant ovarian cancer (A2780T)	[162]
HA5-68	Glycoprotein on A2780T surface	TTAAGGAGCAGCGTGGAGGATATCGG TGTTTATGGTGTCTGTCTTCCTCCAGT TTCCTTCT	PTX-resistant ovarian cancer (A2780T)	[162]
Xq-2-C1	N.A.	CACGGAGGGCTAGAGTAGGGGGCTGT CAAGGGGTCGGTG GGGATATCAGTG	Prostate cancer cell line PC-3M	[163]
U2	Epidermal growth factor receptor variant III (EGFRvIII)	ATCCAGAGTGACGCAGCATTTTGACG CTTTATCCTTTTCTTATGGCGGGATAG TTTCGTGGACACGGTGGCTTAGT	Glioblastoma U87-EGFRvIII cells	[164]
J3	Metastasis related molecules	CCTGAACCTGATGCCAACCTGCCAGC GGGCAGTGCGCGAGTGGGAAACCGA GGGGGACTGAGTAGCGAGCGTGTAGT GTG	Metastatic colorectal carcinoma cell line LoVo, but also PC-3M-1E8, MDA-MB-231	[165]
AB3	Oncofetal antigen/immature laminin receptor protein/ epitope (NQIQAAFREPR) of receptor protein	TGCGTGTGTAGTGTGTCTGTTGTTTGT ATTGTTGTCTATCCTCTTAGGGA TTTGGGCGG	Acute myeloid leukemia	[166]
HB5	HER2/extracellular domain of HER2	AACCGCCCAAATCCCTAAGAGTCTGC ACTTGTCATTTTGTATATGTATTTGGT TTTTGGCTCTCACAGACACACTACAC ACGCACA	HER2-positive breast cancer cells (*e.g*. SK-BR-3)	[167]
Sgc8	Protein tyrosine kinase (PTK7)	ATCTAACTGCTGCGCCGCCGGGAAAA TACTGTACGGTTAGA	Acute lymphoblastic leukemia T cells (CCRF-CEM)	[151,168]
GMT8	N.A.	TGACGAGCCCAAGTTACCTCGATCTT GTGTGTTTAATTGTTTATTGCTGTACC GTGAGAATCTCCGCTGCCTACA	Glioblastoma cell lines A172 and U87MG	[169]
Gint4.T	Platelet-derived growth factor receptor β (PDGFRβ) ectodomain	UGUCGUGGGGCAUCGAGUAAAUGCA AUUCGACA	Human glioblastoma cell lines U87MG and T98G	[170]

AS1411 (formerly known as AGRO100)	Nucleolin	GGTGGTGGTGGTTGTGGTGGTGGTGG	Great variety of cancer cell lines, *e.g.*, MCF7 and MDA-MB-231, U87MG	[171,172]

The aptamer AS1411 is a prominent representative within the group and is often used in "smart" drug delivery devices since it can target different cancer types. It contains 26 nucleotides that form a G-quadruplex, and it binds and inhibits nucleolin. However, its precise mechanism of action and the reason for its cytotoxicity have not yet been fully elucidated [171,172]. Its development over the past 20 years has been extensively reviewed by Bates *et al.* [171,172]. There, the authors address the important issues regarding the mechanism of action when conjugated with drug delivery vehicles [172], since clinical phase II trials of this type (identifier NCT01034410) have been terminated [173]. In this clinical trial, patients with metastatic renal cell carcinoma were treated with the aptamer. It was observed that the treatments have low efficacy with only one out of 35 patients showing a significant response. However, this treatment resulted in a dramatic decrease of tumor lesion, and furthermore, the aptamer showed low toxicity [173].

Investigations of several DNs in combination with AS1411 have already shown promising results [174–177]. By attaching up to three aptamers to a self-assembled pyramidal DNA cage, an increased cell-uptake of the cages in HeLa cells was achieved (Error! Reference source not found.a shows the normalized uptake relative to bare cages) [174]. Increasing the DN concentration or the number of aptamers bound to the cage led to a higher cell uptake. It is suggested that interaction with multiple targets in proximity enhances the uptake. Interestingly, the orientation of the aptamers was found to influence the internalization, which was enhanced when AS1411 was attached to the 3' end of the DNA strands. The nanocarrier inhibited the growth of HeLa cells within 24 h [174]. Improved uptake into tumor cells and co-localization with the nuclei was also observed when only one aptamer was used in combination with cages under hypoxic conditions, resulting in enhanced tumor cell killing of MCF-7 cells [175]. Furthermore, it was shown that the aptamer-equipped cages had an opposite effect on healthy cells, where they could only enter the nuclei in a lesser amount, but the treatment promoted the cell

growth in the healthy tissue of L929 cell lines [175]. These results are promising for the co-delivery of antitumor drugs, like DOX, which could therefore enhance the overall treatment.

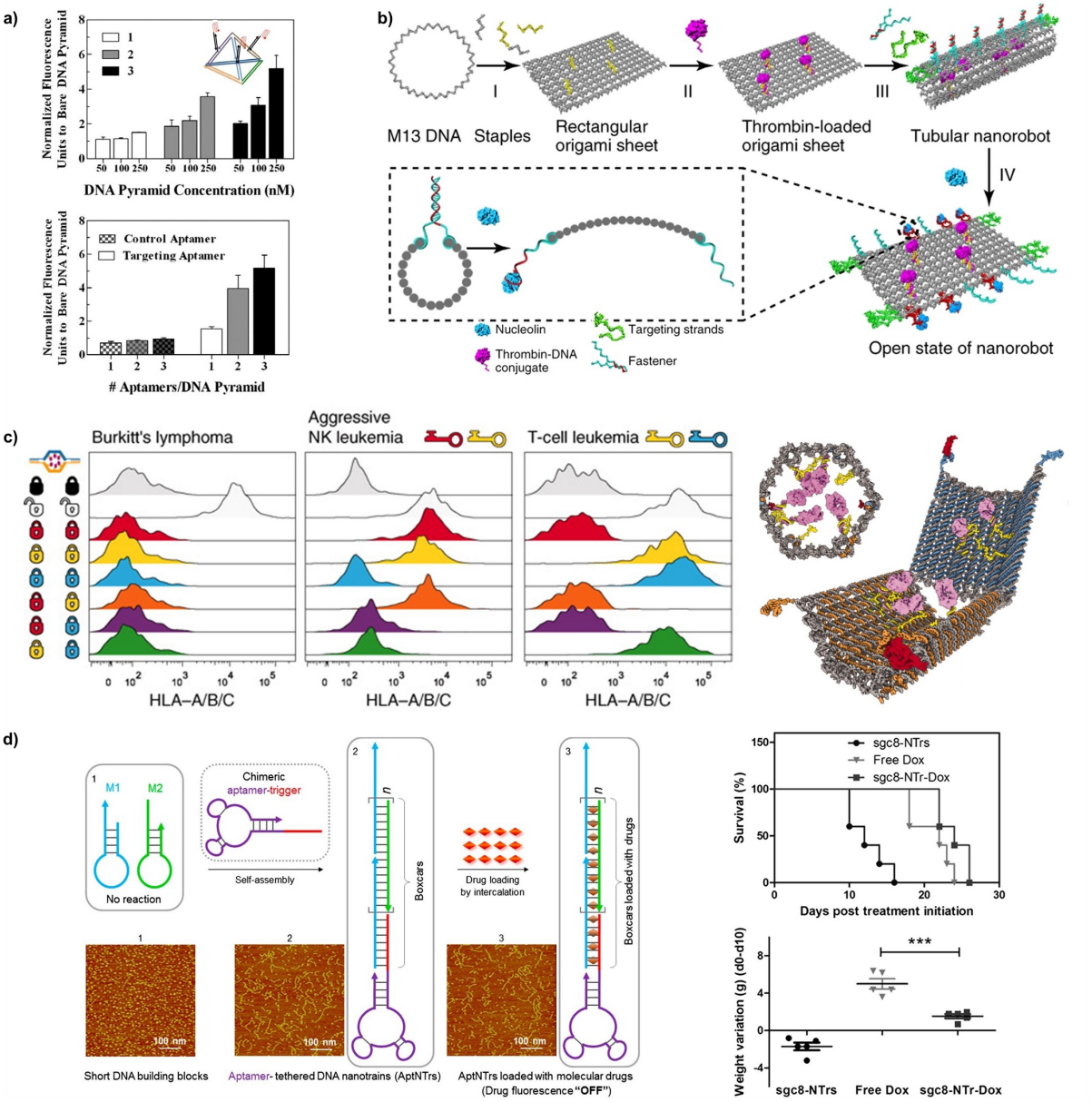

Figure 6. DN devices functionalized with aptamer targeting agents. a) Normalized intracellular uptake of the TDN with 1 to 3 aptamers attached for targeted delivery that is dependent on concentration and number of aptamer strands (top), and in comparison, with nontargeting aptamers (bottom). Adapted with permission [174]. Copyright 2014, American Chemical Society. b) Assembly of the thrombin nanorobot: folding of the DNA sheet (I) with staples (yellow) for thrombin attachment, the attachment of thrombin (II), and assembly into a tubular shape (III) using fastener strands. The closed and opened

states were examined using AFM, the thrombin molecules are displayed as bright spots. Adapted with permission [177]. Copyright 2018, Springer Nature. c) Cell specificity of aptamer-based logic AND gate system due to the cell expression of antigen keys HLA-A/B/C (left); analyzed by flow cytometry by the use of fluorescent anti-HLA-A/B/C antibody fragments. Front and perspective view of the design of the nanorobot (right) with a logic AND gate opening mechanism (orange and blue handles) displaying the payload in form of antibodies (purple) being attached *via* springs (yellow). Adapted with permission [178]. Copyright 2012, The American Association for the Advancement of Science. d) Schematics showing the assembly of aptamer-tethered nanotrains and the morphologies of the building blocks examined with AFM (left). The "boxcar" aptamers (1) are self-assembled and chimeric aptamer-trigger, resulting in aptamer-tethered nanotrains (2) and loaded with drugs (3). Survival of NOD.Cg-Prkdc (scid) IL2 mice employed in the CEM mouse xenograft tumor model (right) upon treatment with free DOX, nanotrains conjugated to the sgc8 aptamer (sgc8-NTr), and sgc8-NTrs loaded with DOX (top), and estimation of the side effects of the treatment by evaluating the weight variation of the mice (bottom). Adapted with permission [179]. Copyright 2013, National Academy of Sciences.

Taghdisi *et al*. [176] used a DOX-loaded three-way junction pocket built from the AS1411 aptamer for the treatment of prostate (PC-3) and breast (4T1) cancer cells. The 3' end of the aptamer was capped with poly(ethylene glycol) (PEG) for enhanced stability. Increased internalization of the drug in cancer cells was obtained, as well as reduced cytotoxicity in healthy cells compared to untargeted treatment [176]. A different strategy for triggering tumor cell death would be starvation, which can be achieved by treatment with thrombin [177]. Thrombin is a blood coagulation protease that catalyses fibrin formation. When delivered to a tumor site, thrombin can induce local fibrin formation, leading to intravascular thrombosis and subsequently inhibition of the tumor growth. This strategy was exploited by employing a thrombin loaded DNA origami nanorobot [177]. By integrating nucleolin-binding aptamers (AS1411) as fastener strands of the closed robot, both targeted delivery and a subsequent opening mechanism were implemented (Error! Reference source not found.b). The system efficiently inhibited tumor growth and metastasis due to thrombin induced fibrin formation, which was observed *in vitro* after the addition

of mouse plasma to the thrombin nanorobot. A cell-induced opening of the device is suggested, since the fibrin formation was twice as fast for samples containing the thrombin nanorobot as in absence of the device. The tumor targeting efficiency was high *in vivo*; after 8 h the greatest accumulation was achieved, which was seven times higher than for a nanorobot without the aptamer. Tests assessing the treatment of MDA-MB231 tumor in mice showed increased survival rates. Furthermore, it was also found to be safe for large animals since thrombosis was not affecting other regions than the tumor tissue [177]. The opening mechanism of such nanodevices can be further refined. Using a hollow, hexagonal barrel shaped nanorobot, Douglas *et al*. [178] delivered multiple payloads, such as gold nanoparticles and antibody fragments anchored to attachment sites on the interior. In order to control the opening of the nanorobot a logic AND gate was implemented using two handles based on the DNA aptamer lock mechanism (**Figure 6**c). Thereby, both antigens need to bind simultaneously to trigger the opening. By combining various aptamer locks, the specificity for different cancer cell types was demonstrated [178].

The RNA aptamer Gint4.T was found to cross the blood-brain barrier and therefore serves as a promising candidate for the treatment of brain tumor, *e.g*. glioblastoma multiforme [170,180,181]. Nanoparticle conjugates with Gint4.T consisting of TDNs and Gint4.T or Gint4.T in combination with GMT8 DNA aptamer, which has a high specificity for U87MG glioblastoma cells, were loaded with DOX [182] and PTX [181]. Both constructs showed enhanced uptake into and cytotoxicity against U87MG cells for DOX, inhibiting the cell cycle and proliferation (DOX) and promoting apoptosis (PTX). Furthermore, the PTX loaded Gint4.T/GMT8 nanoparticle was found to efficiently cross an *in vitro* blood-brain barrier [181]. A different aptamer-based nanodevice termed aptamer-tethered DNA nanotrain (aptNTr, Error! Reference source not found.d, left) was presented by Zhu *et al*. [179], in order to circumvent the inefficient production of aptamer-drug conjugates and limited payload capacity. The nanotrains consisted of “boxcars”, which were short DNA building blocks that assembled into a long linear nanostructure. They were able to carry to carry the chemotherapeutic agents DOX, daunorubucin or epirubicin. The “boxcars” were connected to the aptamer sgc8 for site-specific delivery. The nanodevice showed excellent targeting efficiency and cytotoxicity *in vitro*, as well as inhibition of tumor growth and reduction of DOX side effects *in vivo* (**Figure 6**d, right). It is suggested to serve as a

promising platform for anticancer therapy because of its high drug loading capacity and enhanced circulation time achieved through the linear structure [179].

Often, several different stimuli properties are combined within one system. For instance, by changing the amount of TAT and CGC triplets in the aptamer sequence without affecting the secondary structure the binding affinity of a DNA aptamer towards its target can be controlled by the pH of the solution [183]. Moreover, the pH-dependency can be tuned by the introduction of A^+-C [184] and A^+-G [185] mismatches in the double-stranded region. Adenosine is protonated at low pH and can subsequently form hydrogen bonds with cysteine [186]. The A^+-G mismatch were also found to be formed at acidic pH [185]. By combining both approaches, a strand-displacement -based aptamer with high affinity and an operation environment within a narrow pH range was designed [183]. Even though this approach was facilitated with an ATP-binding aptamer, the authors proposed the compatibility of the concept with other aptamer sequences as well. This would also enable targeting of the ligands during endosomal trafficking, which is associated with the pH decrease [183]. Aptamers can also be combined with other targeting compounds such as small ligand molecules like folic acid [187].

4.3. Small Ligand Molecules, Proteins, and Peptides

Small ligand molecules can mimic antibodies [188], but also target other receptors, like the folate receptor [29,189,190] or the modular transmembrane protein neuropilin-1 [31]. The 2-[3-(1,3-dicarboxy propyl)-ureido] pentanedioic acid (DUPA) is an example of the antibody-mimicking small molecules. Using a specifically designed DNA linker, DUPA was attached to a 6-helix bundle (6HB) DNA origami loaded with DOX. The vehicle exhibited enhanced selectivity and cytotoxicity against $PSMA^+$ (prostate-specific membrane antigen) prostate cancer cells (LNCaP) (**Figure 7**a, top). In comparison to the treatment with free DOX for 48 h at a concentration of 320 nM, which resulted in *ca.* 40% relative cell viability of LNCaP, the DOX-loaded 6HB decorated with DUPA reduced the viability to 20% (Error! Reference source not found.a, bottom). Furthermore, it was shown that the amount of ligands bound to

6HB had an effect on the cytotoxicity, most likely due to the higher possibility of interaction with the target upon increased ligand concentration [188].

On the contrary, cancers of epithelial origin, for instance HeLa cells, can be targeted by folic acid due to the interaction with the overexpressed folate receptor in these cell lines [29]. In combination with DNA tetrahedrons, folic acid has been shown to deliver siRNA *in vivo* to epidermoid carcinoma (KB) tumor xenograft in mice for gene silencing of firefly luciferase (**Figure 7**b, top) [190]. A decrease in *in* vitro cell viability was also observed for a folic acid-octahedral DN loaded with DOX (Error! Reference source not found.b, bottom). While the folate receptor overexpressing HeLa cells showed a significant decrease in cell viability, A431 cells remained unaffected during the treatment. Incubation of the cells with the corresponding concentration (up to 9 μg/mL) of free DOX showed about 65 % cell viability while the lower doses yielded almost 100 % survival of the cells [29].

Receptor-target interactions have also been investigated for the transferrin receptor which is involved in iron transport. Planar DNA origami structures were successfully taken-up by a transferrin receptor overexpressing KB carcinoma cell line [191].

A slightly different targeting approach applies to the cationic peptide D-$(KLAKLAK)_2$, which is known to penetrate tumor cell tissue and target mitochondria, making it an attractive conjugate to DNs. For DOX delivery, the peptide was attached to TDNs (**Figure 7**c, top) at different concentrations, on one to three sites. Endosomal escape during the cell uptake was observed, being more prominent for the TDNs with three cationic peptides due to the destabilization of the membrane by KLA. This nanostructure was also observed to yield the highest DOX release at mitochondria and to subsequently induce cell apoptosis and *in vitro* anticancer efficacy in 4T1 breast cancer cells (Error! Reference source not found.c, bottom) [192]. However, these results may not be so straightforward to interpret as using DOX-DN complexes would require careful consideration of the effective DOX loading and the applied conditions [79].

Apart from specifically designed peptides, widely and commonly available proteins can be used for targeted delivery. Albumin for instance was found to accumulate in tumor tissues, interacting with the cell surface receptor gp60 and the glycoprotein SPARC (secreted protein, acidic and rich in cysteine) [193]. Bovine serum albumin (BSA) includes several reactive sites (Cys34, Lys199, hydrophobic pocket) that enable specific binding/conjugation reactions that can be performed easily, thus making it a rather attractive carrier component [193].

In combination with PTX, albumin (Abraxane®, *nab*®-Paclitaxel) has been approved by the U.S. Food and Drug Administration (FDA) for treatments of metastatic pancreatic cancer, advanced breast cancer and non-small-cell lung cancer [194,195]. Additionally, albumin and virus capsid proteins have been studied to enhance the uptake into cell tissue and increase the stability of DNs [57,196]. Virus mimicking approaches utilize a protecting membrane made of a PEGylated lipid bilayer [197].

Auvinen *et al.* [57] showed that employing BSA-dendron conjugate as a coating material increased DNA origami transfection and simultaneously improved their stability against deoxyribonuclease (DNase) enzymatic degradation. Moreover, cowpea chlorotic mottle virus (CCMV) capsid proteins have been assembled on DNs subsequently enhancing their transfection into human cells (HEK293) [196].

For several other non-mammalian viruses, native tropism has been reported, which means that certain viruses have an affinity to certain cells, and due to a leaky vascular system the coated nanostructures can accumulate in the tumor tissue, making these suitable for active targeting applications [198]. Theiler's murine encephalomyelitis virus (TMEV) binds to the proteins vimentin and desmin of infected BHK-21 cells [199]. Recently, binding of cowpea mosaic virus (CPMV) to surface vimentin was detected, suggesting its potential use in cancer treatment as vimentin is associated with metastasis [200]. The capsid proteins of physalis mottle virus have been equipped with the peptide sequence DGEA [201], which showcases a high affinity towards integrin $\alpha_2\beta_1$ which is overexpressed in PC-3 prostate cancer. Thus,

this peptide sequence (DGEA) has been shown to help in specificity and internalization when conjugated with cell penetrating peptides in prostate cancer cell line [202].

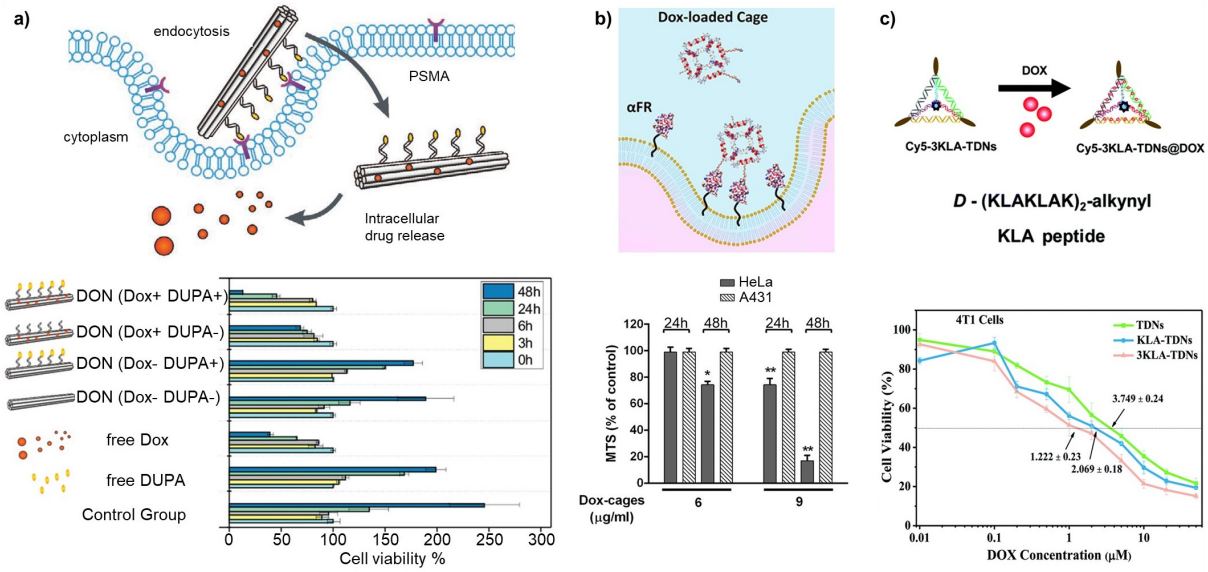

Figure 7. Effect of small molecules/peptides on the viability of tumor cells. a) Working principle of the antibody-mimicking molecule DUPA attached to DON which was loaded with DOX (top). Comparison of cell cytotoxicity of DOX-DUPA-DON (100 nM), DON, DUPA-DON, DOX-DON, and free DOX (320 μM) against LNCaP cells for 0-48 h (bottom). Adapted with permission [188]. Copyright 2020, John Wiley and Sons. b) Graphical representation of DOX-loaded folate-functionalized octahedral DNA nanocages delivering the drug selectively to cancer cells expressing the α isoform of the folate receptor (αFR) (top). Cell viability of HeLa (folate receptor overexpression, grey) and A431 cells upon treatment with DOX loaded octahedral cages modified with folic acid for targeting (bottom). *p<0.05, **p<0.01 Adapted with permission [29]. Copyright 2018, Elsevier. c) Schematic diagram of Cy5-labeled 3KLA-TDNs/DOX (top). Evaluation of anticancer properties of DOX loaded TDNs with 0, 1 or 3 KLA peptides attached against 4T1 cells (bottom). The half-maximal inhibitory concentration is given in μM. Adapted with permission [192]. Copyright 2019, Royal Society of Chemistry.

4.4. Immunostimulation and Vaccines

Immunostimulation provides an intriguing approach in cancer therapeutics by promoting intrinsic defences of the human body against malignant cell growth [203]. Immune response to cancer development

is a complicated and multifaceted process involving multiple branches of immune cells [204]. Here, the focus will be on CpG oligodeoxynucleotides (CpG ODNs) and their use in combination with DNs to activate both the adaptive and the innate immune system to combat tumor growth. CpG ODNs are unmethylated DNA molecules consisting of cytosine (C) triphosphate deoxynucleotide linked to guanine (G) triphosphate deoxynucleotide by phosphodiester (p). CpG ODNs motifs are naturally present in bacterial and viral DNA and once they are exposed during infection, they are detected by the innate immune system cells *via* the Toll-like receptor (TLR) 9, initiating a strong immune response [205,206]. Activation of TLR9 in immune cells, such as plasmacytoid dendritic cells and B cells, actuates a complex signalling cascade which involves the release of multiple cytokines and chemokines [207]. The role of cytokines in stimulation of immune effects cells have been studied in detail and it is already established that they provide increased tumor cell recognition by cytotoxic effector cells [208].

Multiple studies have shown that DNs functionalized with CpG ODNs are able to transfect immune cells and promote cytokine release [32,33,209–211]. Takahashi *et al.* [32] developed a polypodna-like DN functionalized by CpG ODNs for immunostimulation of RAW264.7 murine macrophage-like cells, while Li *et al.* [210] investigated TDNs functionalized with the CpG motif in the same cell line. Both studies showed an efficient transfection and a strong cytokine production in their respective cell lines *in vitro*. However, evidence of the anti-tumorigenic effects of these designs *in vitro* or *in vivo* is still lacking [32,210]. In addition, the appropriateness of these studies regarding the translation to human cells remains still unknown [205].

It is also possible to develop DNA-based nanovaccines against cancer. These vaccines deal with the immunization of the host against malignant cell growth by delivering a payload of immunostimulants to immune cells. Recently, Liu *et. al.* [35] designed a multidrug-loaded, pH-responsive DNA origami nanodevice, which was loaded with the tumor antigen peptide ovalbumin and different TLR agonists (in the form of double-stranded RNA and CpG ODNs) for triggering T cell activation. The cargo was anchored onto certain positions of a DNA origami sheet using short toehold strands, and the DNA

origami sheet was rolled into a tubular structure by closing it with pH-responsive lock strands, which were based on DNA triplexes and could be opened in acidic environment (pH 5.5). In *in vivo* studies conducted in C57BL/6 mice, a prolonged survival (60 % survived for over 40 days) upon nanovaccine treatment was observed compared to the life expectancy (maximum 25 days) without treatment. The presented study revealed promising results regarding both the prolonged survival and the control of tumor growth. Further studies would be warranted to solidify this approach as an efficient way to enhance antitumor activity.

5. Future Prospects and Challenges

Targeted drug delivery in cancer treatment has been introduced as an approach for delivering a higher dose of drug molecules to the tumorous tissue, while simultaneously causing less side effects than traditional chemotherapy [43]. The efficiency of such methods has been verified by employing several DN-based devices, which are either responsive to external stimuli like pH-value, or engineered for specific interactions like proteins or aptamers. In the near future, we envision to see further development of stimuli-responsive and targeted DNs, bringing them closer to clinical use. Here, we have divided the study areas into three topics as outlined in **Figure 8**.

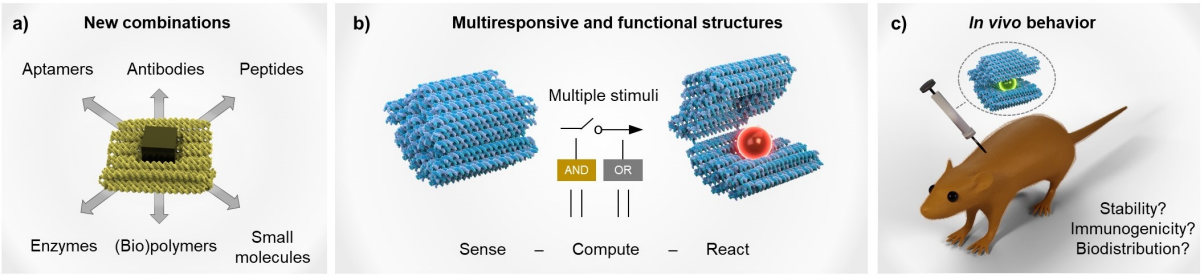

Figure 8: A schematic representation of the future prospects of the DNs in cancer therapies such as (a) novel combinations of DNs with biomolecules (b) multi-responsive and functional structures triggered based on logic gates or multi-stimuli and (c) *in vivo* drug behavior and response of DN-based therapeutics.

5.1. New Combinations of DNs and Other Biomolecules

As presented in this review, DNs can be efficiently combined with other biomolecules and nucleic acids to yield hybrid structures with programmable functions. In addition, the diversity of DN designs and combinations of DNs and other pivotal biomolecules can be expected to increase. This may yield enhanced targeting functions through either binding to target molecules or through specific responses to physical or chemical stimuli, or increase the stability of DNs in the physiological environment.

Aptamers in particular present a very promising and versatile approach for targeting. Since unmodified aptamers are easily degraded by cellular nucleases [139,140] in the physiological environment, complexation with DNs can both help to prevent the enzymatic degradation and also lead to more pronounced effects through the optional drug loading of DNs. The aptamer AS1411 has been used in several studies in combination with DNs, although its clinical trial had to be terminated in Phase II [173]. Several other currently existing aptamers (*e.g.*, NOX-A12 and pegaptanib) that are approved by the US FDA for different therapies, could also be combined with DNs and studied for their improved selectivity resulting in a likely synergistic effect. The NOX-A12 is an orphan drug used in combination with radiotherapy for the treatment of glioblastoma [212], whereas pegaptanib (Macugen) interacts with the vascular endothelial growth factor and is suspected to be effective against solid tumors with extensive angiogenesis [212,213]. With the help of cell-SELEX, the identification of novel aptamers against different types of cancer cells has been commercialized, thus streamlining the development of new potential targeting agents to be combined with DNs. This could pave the way for the development of personalized therapies; however, the clinical potential has to be further stringently assessed.

5.2. Multifunctional Structures and Optimized Responses

Combining environment-based stimuli with design-based targeting agents, or different targeting groups with each other, can also lead to new types of synergistic effects. For instance, aptamers could be combined with cationic peptides, which can also target cancer cells [192,214]. The aptamers and peptides

can interact with different targets on a cell, further increasing the specificity. Nowadays, protein engineering provides a toolbox for the development of proteins and peptides with several distinct properties to further improve the drug delivery. A multi-stimuli nano-system could also be designed based on the work by Thompson *et al.* [183], which showcases how an ATP aptamer can be converted into a pH sensitive switch, thereby having both environment and design-based responses.

DNs eliciting conformational changes upon pH gradient still requires robust biomedical research and further advancement in the field. Most of the reviewed studies have focused on developing pH-responsive DNs that respond to the acidic environment in the lysosome, however, this would require previous internalization of the nanoparticles. Nevertheless, the reverse pH behavior of cancer cells [110] offers a novel and promising approach for targeted delivery. Therefore, devices highly responsive to minimal environmental changes are required, similar to the DNA origami nanocapsule developed by Ijäs *et. al* [116]. The current devices targeting the microenvironment suffer from lack of rigorous research, but we would expect this to be an emerging field of research in the upcoming years. The lack of cell studies also accounts for temperature sensitive devices, although the possibility of designing highly tunable lock sequences has already been presented [121]. For further refinement of the drug release, a logic gate system similar to the nanorobot presented by Douglas *et al.* [178] could be implemented. Such a system could, for instance, include pH-locks for the opening of the device and a pH-sensitive anchor for a bound drug. This would not only minimize the potential drug leakage, but also ensure a multi-step and sustainable release profile.

5.3. Improved Understanding of the *In Vivo* Behavior

As discussed in Section 2.1., one of the main limitations of DNs in clinical use is their limited structural stability under the physical, chemical, and biological destabilizing factors of the physiological environment. The ongoing research on understanding and improving the stability, biocompatibility, and biodistribution of DNs is thus a key in the development of efficient and safe cancer therapeutics.

Many *in vitro* studies have been performed using 2D cell cultures. This monolayer of cells does not truly mimic the tumor complexities, and therefore it would be important to also test the DNs in 3D cell culture models such as multicellular tumor spheroids which allow for investigation of the microenvironment of tumors.[215]. These 3D models can provide a low cost bridge between *in vitro* and *in vivo* studies for evaluating the efficacy of stimuli-based DNs in a more robust way [216].

Certain cancer types, like glioblastoma, are challenging to treat due to the biological barriers, such as the blood-brain barrier. The small size of DNs in combination with appropriate targeting sequences appears to be a rather promising option. There is evidence that DNs can be delivered through the blood-brain barrier, by showing that Gint4.T/GMT8 conjugated with TDNs is able to cross an *in vitro* brain barrier [181]. Similar studies need to be carried out for better understanding of the full potential of DNs as carriers capable of passing the blood-brain barrier.

6. Conclusions

Over the last four decades, major strides have been achieved in the field of DNA nanotechnology. The development of stimuli-based therapies with DNs holds a prominent position in the forthcoming treatment options for a variety of diseases with a specific focus on cancer. This review highlights the applicability of DNs upon targeted delivery based on environmental stimuli and specific ligand-target interactions. Moreover, analysis of the advantages of DNA-based nanocarriers and a brief description of the cell internalization strategies is provided. Several *in vitro* studies have shown enhanced cytotoxicity of drug-loaded nanostructures against different types of cancer cells in comparison to the free drug alone. Studies performed *in vivo* with xenograft mouse models have likewise shown that drug-loaded DNs may cause fewer side effects because of their higher potency, and subsequently, the lower dose required for the treatment. Put together, the results suggest that the nanostructures are indeed an excellent choice for further studies. Controlling the release of drugs with specific stimuli not only improves specificity for their target but also provides, in combination with DNs, new avenues for

treating sturdy drug-resistant cancer types due to the nanostructures' capacity to co-load and co-deliver multiple drugs.

There are still several challenges that need to be tackled to achieve the full potential of DNs in biomedicine. Recent research has been focused on synthesizing these nanoscale structures at large scale, and major advances have been made to develop low-cost and robust scale-up methods [70], similar to other drug delivery systems, for example, liposomes. Nevertheless, even with the lab-scale methods that are easily accessible and widely available, DNs have proven to be efficient in delivery, targeting and dosing, and therefore, also in harnessing the full potential of drugs they are combined with.

AUTHOR INFORMATION

Corresponding Authors

*Email: mauri.kostiainen@aalto.fi

*Email: veikko.linko@aalto.fi

ORCID

Iris Seitz: 0000-0001-6552-9894

Ahmed Shaukat: 0000-0001-9108-0912

Heini Ijäs: 0000-0001-7880-332X

Jouni Hirvonen: 0000-0002-5029-1657

Hélder A. Santos: 0000-0001-7850-6309

Mauri A. Kostiainen: 0000-0002-8282-2379

Veikko Linko: 0000-0003-2762-1555

Author Contributions

⊥ I.S., A.S. and K.N. contributed equally.

Notes

The authors declare no competing financial interests.

ACKNOWLEDGMENT

Financial support by the Emil Aaltonen Foundation, the Sigrid Jusélius Foundation, the Magnus Ehrnrooth Foundation, Academy of Finland (grants no. 317042 and 331151), the Jane and Aatos Erkko Foundation and the Vilho, Yrjö and Kalle Väisälä Foundation of the Finnish Academy of Science and Letters is gratefully acknowledged.

REFERENCES

[1] J. Wolfram, M. Ferrari, *Nano Today* **2019**, *25*, 85.
[2] G. J. Kim, S. Nie, *Mater. Today* **2005**, *8*, 28.
[3] A. Ahmad, F. Khan, R. K. Mishra, R. Khan, *J. Med. Chem.* **2019**, *62*, 10475.
[4] A. Ediriwickrema, W. M. Saltzman, *ACS Biomater. Sci. Eng.* **2015**, *1*, 64.
[5] V. Balasubramanian, Z. Liu, J. Hirvonen, H. A. Santos, *Adv. Healthc. Mater.* **2018**, *7*, 1700432.
[6] J. Fang, H. Nakamura, H. Maeda, *Adv. Drug Deliver. Rev.* **2011**, *63*, 136.
[7] H. Maeda, J. Wu, T. Sawa, Y. Matsumura, K. Hori, *J Control Release* **2000**, *65*, 271.
[8] *Nat. Mater.* **2020**, *19*, 477.
[9] L. Zhou, H. Wang, Y. Li, *Theranostics* **2018**, *8*, 1059.
[10] Y. Qiao, J. Wan, L. Zhou, W. Ma, Y. Yang, W. Luo, Z. Yu, H. Wang, *WIREs Nanomed. Nanobi.* **2019**, *11*, e1527.
[11] C. Vergallo, M. N. Hafeez, D. Iannotta, H. A. Santos, N. D'Avanzo, L. Dini, F. Cilurzo, M. Fresta, L. Di Marzio, C. Christian, in *Bio-Nanomedicine for Cancer Therapy* (Eds: F. Fontana, H. A. Santos), Springer International Publishing, Cham, **2021**, pp. 3–27.
[12] Y. Peng, J. Bariwal, V. Kumar, C. Tan, R. I. Mahato, *Adv. Ther.* **2020**, *3*, 1900136.
[13] G. Hong, S. Diao, A. L. Antaris, H. Dai, *Chem. Rev.* **2015**, *115*, 10816.
[14] H. Wang, Q. Chen, S. Zhou, *Chem. Soc. Rev.* **2018**, *47*, 4198.
[15] S. Bhaskar, S. Lim, *Npg Asia Mater.* **2017**, *9*, e371.
[16] M. Karimi, P. S. Zangabad, F. Mehdizadeh, H. Malekzad, A. Ghasemi, S. Bahrami, H. Zare, M. Moghoofei, A. Hekmatmanesh, M. R. Hamblin, *Nanoscale* **2017**, *9*, 1356.
[17] X. Qin, Y. Li, *ChemBioChem* **2020**, *21*, 1236.

[18] S. Lu, J. Shen, C. Fan, Q. Li, X. Yang, *Adv. Sci.* **2021**, *n/a*, 2100328.
[19] A. García-Fernández, E. Aznar, R. Martínez-Máñez, F. Sancenón, *Small* **2020**, *16*, 1902242.
[20] R. S. Guimarães, C. F. Rodrigues, A. F. Moreira, I. J. Correia, *Pharmacol. Res.* **2020**, *155*, 104742.
[21] J. Chen, N. C. Seeman, *Nature* **1991**, *350*, 631.
[22] P. W. K. Rothemund, *Nature* **2006**, *440*, 297.
[23] P. Wang, T. A. Meyer, V. Pan, P. K. Dutta, Y. Ke, *Chem* **2017**, *2*, 359.
[24] S. Nummelin, J. Kommeri, M. A. Kostiainen, V. Linko, *Adv. Mater.* **2018**, *30*, 1703721.
[25] X. Chen, T. Chen, L. Ren, G. Chen, X. Gao, G. Li, X. Zhu, *ACS Nano* **2019**, *13*, 7333.
[26] Y.-F. Chen, M.-W. Hsu, Y.-C. Su, H.-M. Chang, C.-H. Chang, J.-S. Jan, *Mater. Sci. Eng. C* **2020**, *114*, 111025.
[27] F. Huang, W.-C. Liao, Y. S. Sohn, R. Nechushtai, C.-H. Lu, I. Willner, *J. Am. Chem. Soc.* **2016**, *138*, 8936.
[28] G. J. Lee, T. Kim, *Pharmaceutics* **2019**, *11*, 247.
[29] S. Raniolo, G. Vindigni, A. Ottaviani, V. Unida, F. Iacovelli, A. Manetto, M. Figini, L. Stella, A. Desideri, S. Biocca, *Nanomedicine* **2018**, *14*, 1181.
[30] G.-Y. Sun, Y.-C. Du, Y.-X. Cui, J. Wang, X.-Y. Li, A.-N. Tang, D.-M. Kong, *ACS Appl. Mater. Interfaces* **2019**, *11*, 14684.
[31] Z. Xia, P. Wang, X. Liu, T. Liu, Y. Yan, J. Yan, J. Zhong, G. Sun, D. He, *Biochemistry* **2016**, *55*, 1326.
[32] Y. Takahashi, T. Maezawa, Y. Araie, Y. Takahashi, Y. Takakura, M. Nishikawa, *J. Pharm. Sci.* **2017**, *106*, 2457.
[33] Y. Qu, Y. Ju, C. Cortez-Jugo, Z. Lin, S. Li, J. Zhou, Y. Ma, A. Glab, S. J. Kent, F. Cavalieri, et al., *Small* **2020**, *16*, 2002750.
[34] Q. Jiang, Y. Shi, Q. Zhang, N. Li, P. Zhan, L. Song, L. Dai, J. Tian, Y. Du, Z. Cheng, et al., *Small* **2015**, *11*, 5134.
[35] S. Liu, Q. Jiang, X. Zhao, R. Zhao, Y. Wang, Y. Wang, J. Liu, Y. Shang, S. Zhao, T. Wu, et al., *Nat. Mater.* **2021**, *20*, 421.
[36] M. I. Setyawati, R. V. Kutty, D. T. Leong, *Small* **2016**, *12*, 5601.
[37] Y. Yao, Y. Zhou, L. Liu, Y. Xu, Q. Chen, Y. Wang, S. Wu, Y. Deng, J. Zhang, A. Shao, *Front. Mol. Biosci.* **2020**, *7*, 193.
[38] Y. Li, X. Zheng, Q. Chu, *Nano Today* **2021**, *38*, 101134.
[39] A. Sanginario, B. Miccoli, D. Demarchi, *Biosensors* **2017**, *7*, 9.
[40] R. Duangrat, A. Udomprasert, T. Kangsamaksin, *Cancer Sci.* **2020**, *111*, 3164.
[41] M. D. Massich, D. A. Giljohann, D. S. Seferos, L. E. Ludlow, C. M. Horvath, C. A. Mirkin, *Mol. Pharmaceut.* **2009**, *6*, 1934.
[42] J. Li, C. Fan, H. Pei, J. Shi, Q. Huang, *Adv. Mater. Weinheim* **2013**, *25*, 4386.
[43] R. V. J. Chari, M. L. Miller, W. C. Widdison, *Angew. Chem. Int. Ed.* **2014**, *53*, 3796.
[44] X. Ouyang, M. De Stefano, A. Krissanaprasit, A. L. Bank Kodal, C. Bech Rosen, T. Liu, S. Helmig, C. Fan, K. V. Gothelf, *Angew. Chem. Int. Ed.* **2017**, *56*, 14423.
[45] Q. Jiang, C. Song, J. Nangreave, X. Liu, L. Lin, D. Qiu, Z.-G. Wang, G. Zou, X. Liang, H. Yan, et al., *J. Am. Chem. Soc.* **2012**, *134*, 13396.
[46] J. Hahn, S. F. J. Wickham, W. M. Shih, S. D. Perrault, *ACS Nano* **2014**, *8*, 8765.
[47] Q. Mei, X. Wei, F. Su, Y. Liu, C. Youngbull, R. Johnson, S. Lindsay, H. Yan, D. Meldrum, *Nano Letters* **2011**, *11*, 1477.
[48] A. Heuer-Jungemann, P. K. Harimech, T. Brown, A. G. Kanaras, *Nanoscale* **2013**, *5*, 9503.
[49] A. R. Chandrasekaran, *Nat Rev Chem* **2021**, *5*, 225.

[50] C. Kielar, Y. Xin, B. Shen, M. A. Kostiainen, G. Grundmeier, V. Linko, A. Keller, *Angew. Chem. Int. Ed.* **2018**, *57*, 9470.
[51] J.-W. Keum, H. Bermudez, *Chem. Commun.* **2009**, 7036.
[52] N. C. Seeman, *J. Theor. Biol.* **1982**, *99*, 237.
[53] A. R. Chandrasekaran, J. Vilcapoma, P. Dey, S. W. Wong-Deyrup, B. K. Dey, K. Halvorsen, *J. Am. Chem. Soc.* **2020**, *142*, 6814.
[54] K.-R. Kim, H. Y. Kim, Y.-D. Lee, J. S. Ha, J. H. Kang, H. Jeong, D. Bang, Y. T. Ko, S. Kim, H. Lee, et al., *J. Control. Release* **2016**, *243*, 121.
[55] C. E. Castro, F. Kilchherr, D.-N. Kim, E. L. Shiao, T. Wauer, P. Wortmann, M. Bathe, H. Dietz, *Nat. Methods* **2011**, *8*, 221.
[56] J. W. Conway, C. K. McLaughlin, K. J. Castor, H. Sleiman, *Chem. Commun.* **2013**, *49*, 1172.
[57] H. Auvinen, H. Zhang, Nonappa, A. Kopilow, E. H. Niemelä, S. Nummelin, A. Correia, H. A. Santos, V. Linko, M. A. Kostiainen, *Adv. Healthc. Mater.* **2017**, *6*, 1700692.
[58] J. K. Kiviaho, V. Linko, A. Ora, T. Tiainen, E. Järvihaavisto, J. Mikkilä, H. Tenhu, N. Nonappa, M. A. Kostiainen, *Nanoscale* **2016**, *8*, 11674.
[59] N. Ponnuswamy, M. M. C. Bastings, B. Nathwani, J. H. Ryu, L. Y. T. Chou, M. Vinther, W. A. Li, F. M. Anastassacos, D. J. Mooney, W. M. Shih, *Nat. Comm.* **2017**, *8*, 15654.
[60] N. P. Agarwal, M. Matthies, F. N. Gür, K. Osada, T. L. Schmidt, *Angew. Chem. Int. Ed.* **2017**, *56*, 5460.
[61] S. Mishra, Y. Feng, M. Endo, H. Sugiyama, *ChemBioChem* **2020**, *21*, 33.
[62] N. Stephanopoulos, *ChemBioChem* **2019**, *20*, 2191.
[63] A. Keller, V. Linko, *Angew. Chem. Int. Ed.* **2020**, *59*, 15818.
[64] S. Ramakrishnan, H. Ijäs, V. Linko, A. Keller, *Comput. Struct. Biotechnol.* **2018**, *16*, 342.
[65] H. Bila, E. E. Kurisinkal, M. M. C. Bastings, *Biomater. Sci.* **2019**, *7*, 532.
[66] M. Madsen, K. V. Gothelf, *Chem. Rev.* **2019**, *119*, 6384.
[67] A. Shaw, E. Benson, B. Högberg, *ACS Nano* **2015**, *9*, 4968.
[68] A. Cherepanova, S. Tamkovich, D. Pyshnyi, M. Kharkova, V. Vlassov, P. Laktionov, *J. Immunol. Methods* **2007**, *325*, 96.
[69] E. L. Coleridge, K. E. Dunn, *Biomed. Phys. Eng. Express* **2020**, *6*, 065030.
[70] F. Praetorius, B. Kick, K. L. Behler, M. N. Honemann, D. Weuster-Botz, H. Dietz, *Nature* **2017**, *552*, 84.
[71] D. Gewirtz, *Biochem. Pharmacol.* **1999**, *57*, 727.
[72] D. Agudelo, P. Bourassa, G. Bérubé, H.-A. Tajmir-Riahi, *Int. J. Biol. Macromol.* **2014**, *66*, 144.
[73] V. G. S. Box, *J. Mol. Graph. Model.* **2007**, *26*, 14.
[74] S. M. Taghdisi, N. M. Danesh, M. Ramezani, R. Yazdian-Robati, K. Abnous, *Mol. Pharmaceutics* **2018**, *15*, 1972.
[75] M. Chang, C.-S. Yang, D.-M. Huang, *ACS Nano* **2011**, *5*, 6156.
[76] K. Abnous, N. M. Danesh, M. Ramezani, F. Charbgoo, A. Bahreyni, S. M. Taghdisi, *Expert Opin. Drug Del.* **2018**, *15*, 1045.
[77] Y. Zeng, J. Liu, S. Yang, W. Liu, L. Xu, R. Wang, *J. Mater. Chem. B* **2018**, *6*, 1605.
[78] Q. Zhang, Q. Jiang, N. Li, L. Dai, Q. Liu, L. Song, J. Wang, Y. Li, J. Tian, B. Ding, et al., *ACS Nano* **2014**, *8*, 6633.
[79] H. Ijäs, B. Shen, A. Heuer-Jungemann, A. Keller, M. A. Kostiainen, T. Liedl, J. A. Ihalainen, V. Linko, *Nucleic Acids Res.* **2021**, *49*, 3048.

[80] Y.-X. Zhao, A. Shaw, X. Zeng, E. Benson, A. M. Nyström, B. Högberg, *ACS Nano* **2012**, *6*, 8684.
[81] Y. Ke, G. Bellot, N. V. Voigt, E. Fradkov, W. M. Shih, *Chem. Sci.* **2012**, *3*, 2587.
[82] H. L. Miller, S. Contera, A. J. M. Wollman, A. Hirst, K. E. Dunn, S. Schröter, D. O'Connell, M. C. Leake, *Nanotechnology* **2020**, *31*, 235605.
[83] P. D. Halley, C. R. Lucas, E. M. McWilliams, M. J. Webber, R. A. Patton, C. Kural, D. M. Lucas, J. C. Byrd, C. E. Castro, *Small* **2016**, *12*, 308.
[84] C. Zhang, H. Zhang, M. Han, X. Yang, C. Pei, Z. Xu, J. Du, W. Li, S. Chen, *RSC Adv.* **2019**, *9*, 1982.
[85] M. Abbas, M. M. F. A. Baig, Y. Zhang, Y.-S. Yang, S. Wu, Y. Hu, Z.-C. Wang, H.-L. Zhu, *J. Pharm. Anal.* **2020**, DOI 10.1016/j.jpha.2020.03.005.
[86] T. Wu, J. Liu, M. Liu, S. Liu, S. Zhao, R. Tian, D. Wei, Y. Liu, Y. Zhao, H. Xiao, et al., *Angew. Chem. Int. Ed.* **2019**, *58*, 14224.
[87] Y. Zhong, J. Cheng, Y. Liu, T. Luo, Y. Wang, K. Jiang, F. Mo, J. Song, *Small* **2020**, *16*, 2003646.
[88] W. A. Hammond, A. Swaika, K. Mody, *Ther Adv Med Oncol* **2016**, *8*, 57.
[89] E. Chu, D. M. Koeller, P. G. Johnston, S. Zinn, C. J. Allegra, *Mol. Pharmacol.* **1993**, *43*, 527.
[90] R. B. Diasio, B. E. Harris, *Clin Pharmacokinet* **1989**, *16*, 215.
[91] A. F. Jorge, A. Aviñó, A. A. C. C. Pais, R. Eritja, C. Fàbrega, *Nanoscale* **2018**, *10*, 7238.
[92] S. Alcaro, D. Battaglia, F. Ortuso, *Il Farmaco* **2003**, *58*, 691.
[93] G. Bischoff, U. Gromann, S. Lindau, W. V. Meister, S. Hoffmann, *Nucleos. Nucleot.* **1999**, *18*, 2201.
[94] X. Xie, X. Shao, W. Ma, D. Zhao, S. Shi, Q. Li, Y. Lin, *Nanoscale* **2018**, *10*, 5457.
[95] F. Kollmann, S. Ramakrishnan, B. Shen, G. Grundmeier, M. A. Kostiainen, V. Linko, A. Keller, *ACS Omega* **2018**, *3*, 9441.
[96] M. M. C. Bastings, F. M. Anastassacos, N. Ponnuswamy, F. G. Leifer, G. Cuneo, C. Lin, D. E. Ingber, J. H. Ryu, W. M. Shih, *Nano Lett.* **2018**, *18*, 3557.
[97] T. Maezawa, S. Ohtsuki, K. Hidaka, H. Sugiyama, M. Endo, Y. Takahashi, Y. Takakura, M. Nishikawa, *Nanoscale* **2020**, *12*, 14818.
[98] P. Wang, M. A. Rahman, Z. Zhao, K. Weiss, C. Zhang, Z. Chen, S. J. Hurwitz, Z. G. Chen, D. M. Shin, Y. Ke, *J. Am. Chem. Soc.* **2018**, *140*, 2478.
[99] G. Chen, D. Liu, C. He, T. R. Gannett, W. Lin, Y. Weizmann, *J. Am. Chem. Soc.* **2015**, *137*, 3844.
[100] A. Lacroix, E. Vengut-Climent, D. de Rochambeau, H. F. Sleiman, *ACS Cent. Sci.* **2019**, *5*, 882.
[101] L. Liang, J. Li, Q. Li, Q. Huang, J. Shi, H. Yan, C. Fan, *Angew. Chem. Int. Ed.* **2014**, *53*, 7745.
[102] H. Ding, J. Li, N. Chen, X. Hu, X. Yang, L. Guo, Q. Li, X. Zuo, L. Wang, Y. Ma, *ACS Cent. Sci.* **2018**, *4*, 1344.
[103] M. A. Rahman, P. Wang, Z. Zhao, D. Wang, S. Nannapaneni, C. Zhang, Z. Chen, C. C. Griffith, S. J. Hurwitz, Z. G. Chen, *Angew. Chem. Int. Ed.* **2017**, *56*, 16023.
[104] C. M. Green, D. Mathur, I. L. Medintz, *J. Mater. Chem. B* **2020**, *8*, 6170.
[105] G. Vindigni, S. Raniolo, A. Ottaviani, M. Falconi, O. Franch, B. R. Knudsen, A. Desideri, S. Biocca, *ACS Nano* **2016**, *10*, 5971.
[106] J. H. Kang, K.-R. Kim, H. Lee, D.-R. Ahn, Y. T. Ko, *Colloid Surface B* **2017**, *157*, 424.
[107] X. Shen, Q. Jiang, J. Wang, L. Dai, G. Zou, Z.-G. Wang, W.-Q. Chen, W. Jiang, B. Ding, *Chem. Commun.* **2012**, *48*, 11301.

[108] R. Shi, L. Huang, X. Duan, G. Sun, G. Yin, R. Wang, J. Zhu, *Anal. Chim. Acta* **2017**, *988*, 66.
[109] L. Song, V. H. B. Ho, C. Chen, Z. Yang, D. Liu, R. Chen, D. Zhou, *Adv. Healthc. Mater.* **2013**, *2*, 275.
[110] K. A. White, B. K. Grillo-Hill, D. L. Barber, *J Cell Sci* **2017**, *130*, 663.
[111] O. Warburg, F. Wind, E. Negelein, *J. Gen. Physiol.* **1927**, *8*, 519.
[112] V. Estrella, T. Chen, M. Lloyd, J. Wojtkowiak, H. H. Cornnell, A. Ibrahim-Hashim, K. Bailey, Y. Balagurunathan, J. M. Rothberg, B. F. Sloane, et al., *Cancer Res* **2013**, *73*, 1524.
[113] H. Zhang, X. Qu, H. Chen, H. Kong, R. Ding, D. Chen, X. Zhang, H. Pei, H. A. Santos, M. Hai, et al., *Adv. Healthc. Mater.* **2017**, *6*, 1700664.
[114] A. R. Chandrasekaran, D. A. Rusling, *Nucleic Acids Res.* **2018**, *46*, 1021.
[115] A. Idili, A. Vallée-Bélisle, F. Ricci, *J. Am. Chem. Soc.* **2014**, *136*, 5836.
[116] H. Ijäs, I. Hakaste, B. Shen, M. A. Kostiainen, V. Linko, *ACS Nano* **2019**, *13*, 5959.
[117] D. E. Meyer, B. C. Shin, G. A. Kong, M. W. Dewhirst, A. Chilkoti, *J. Control. Release* **2001**, *74*, 213.
[118] V. A. Turek, R. Chikkaraddy, S. Cormier, B. Stockham, T. Ding, U. F. Keyser, J. J. Baumberg, *Adv. Funct. Mater.* **2018**, *28*, 1706410.
[119] S. Juul, F. Iacovelli, M. Falconi, S. L. Kragh, B. Christensen, R. Frøhlich, O. Franch, E. L. Kristoffersen, M. Stougaard, K. W. Leong, et al., *ACS Nano* **2013**, *7*, 9724.
[120] O. Franch, F. Iacovelli, M. Falconi, S. Juul, A. Ottaviani, C. Benvenuti, S. Biocca, Y.-P. Ho, B. R. Knudsen, A. Desideri, *Nanoscale* **2016**, *8*, 13333.
[121] D. Gareau, A. Desrosiers, A. Vallée-Bélisle, *Nano Lett.* **2016**, *16*, 3976.
[122] Z. Yu, N. Li, P. Zheng, W. Pan, B. Tang, *Chem. Commun.* **2014**, *50*, 3494.
[123] A. Shaukat, E. Anaya-Plaza, S. Julin, V. Linko, T. Torres, A. de la Escosura, M. A. Kostiainen, *Chem. Commun.* **2020**, *56*, 7341.
[124] P. Singh, S. Pandit, V. R. S. S. Mokkapati, A. Garg, V. Ravikumar, I. Mijakovic, *Int J Mol Sci* **2018**, *19*, DOI 10.3390/ijms19071979.
[125] Z.-Z. J. Lim, J.-E. J. Li, C.-T. Ng, L.-Y. L. Yung, B.-H. Bay, *Acta Pharmacol. Sin.* **2011**, *32*, 983.
[126] Y. Du, Q. Jiang, N. Beziere, L. Song, Q. Zhang, D. Peng, C. Chi, X. Yang, H. Guo, G. Diot, et al., *Adv. Mater.* **2016**, *28*, 10000.
[127] F. Kong, H. Zhang, X. Qu, X. Zhang, D. Chen, R. Ding, E. Mäkilä, J. Salonen, H. A. Santos, M. Hai, *Adv. Mater.* **2016**, *28*, 10195.
[128] K. Abnous, N. M. Danesh, M. Ramezani, M. Alibolandi, A. Bahreyni, P. Lavaee, S. A. Moosavian, S. M. Taghdisi, *J. Drug. Target.* **2020**, *28*, 852.
[129] L. Feng, Y. Cai, M. Zhu, L. Xing, X. Wang, *Cancer Cell Int.* **2020**, *20*, 110.
[130] A. Trautmann, *Sci. Signal.* **2009**, *2*, pe6.
[131] S. Yang, Z. Ren, M. Chen, Y. Wang, B. You, W. Chen, C. Qu, Y. Liu, X. Zhang, *Mol. Pharmaceutics* **2018**, *15*, 314.
[132] V. Chudasama, A. Maruani, S. Caddick, *Nature Chem* **2016**, *8*, 114.
[133] E. L. Sievers, P. D. Senter, *Annu. Rev. Med.* **2013**, *64*, 15.
[134] E. W. Orava, N. Cicmil, J. Gariépy, *BBA-Biomembranes* **2010**, *1798*, 2190.
[135] D. Zahavi, L. Weiner, *Antibodies* **2020**, *9*, 34.
[136] B. J. H. M. Rosier, G. A. O. Cremers, W. Engelen, M. Merkx, L. Brunsveld, T. F. A. de Greef, *Chem. Commun.* **2017**, *53*, 7393.
[137] J. Z. Hui, S. Tamsen, Y. Song, A. Tsourkas, *Bioconjugate Chem.* **2015**, *26*, 1456.
[138] G. A. O. Cremers, B. J. H. M. Rosier, A. Meijs, N. B. Tito, S. M. J. van Duijnhoven, H. van Eenennaam, L. Albertazzi, T. F. A. de Greef, (Preprint) *bioRxiv 02.24.432702*, Feb **2021**.

[139] V. Thiviyanathan, D. G. Gorenstein, *Prot. Clin. Appl.* **2012**, *6*, 563.
[140] A. D. Keefe, S. Pai, A. Ellington, *Nat Rev Drug Discov* **2010**, *9*, 537.
[141] J. K. H. Liu, *Ann. Med. Surg.* **2014**, *3*, 113.
[142] P. W. Barone, M. E. Wiebe, J. C. Leung, I. T. M. Hussein, F. J. Keumurian, J. Bouressa, A. Brussel, D. Chen, M. Chong, H. Dehghani, et al., *Nat Biotechnol* **2020**, *38*, 563.
[143] S. Loisel, M. Ohresser, M. Pallardy, D. Daydé, C. Berthou, G. Cartron, H. Watier, *Crit. Rev. Oncol. Hematol.* **2007**, *62*, 34.
[144] T. Yokota, D. E. Milenic, M. Whitlow, J. Schlom, *Cancer Res* **1992**, *52*, 3402.
[145] M. Wikman, A.-C. Steffen, E. Gunneriusson, V. Tolmachev, G. P. Adams, J. Carlsson, S. Ståhl, *Protein Eng. Des. Sel.***2004**, *17*, 455.
[146] Y. Zhang, S. Jiang, D. Zhang, X. Bai, S. M. Hecht, S. Chen, *Chem. Commun.* **2017**, *53*, 573.
[147] C. Zhang, M. Han, F. Zhang, X. Yang, J. Du, H. Zhang, W. Li, S. Chen, *IJN* **2020**, *Volume 15*, 885.
[148] M. Chu, J. Kang, W. Wang, H. Li, J. Feng, Z. Chu, M. Zhang, L. Xu, Y. Wang, *Cell Mol Immunol* **2017**, *14*, 398.
[149] A. D. Ellington, J. W. Szostak, *Nature* **1990**, *346*, 818.
[150] C. Tuerk, L. Gold, *Science* **1990**, *249*, 505.
[151] D. Shangguan, Y. Li, Z. Tang, Z. C. Cao, H. W. Chen, P. Mallikaratchy, K. Sefah, C. J. Yang, W. Tan, *P. Natl. Acad. Sci.***2006**, *103*, 11838.
[152] J. C. Graham, H. Zarbl, *PLoS ONE* **2012**, *7*, e36103.
[153] X. Yang, *Nucleic Acids Res.* **2002**, *30*, 132e.
[154] B. Santosh, P. K. Yadava, *Biomed Res. Int.* **2014**, *2014*, 1.
[155] H. Kaur, *BBA-Gen. Subjects* **2018**, *1862*, 2323.
[156] X. Li, Y. An, J. Jin, Z. Zhu, L. Hao, L. Liu, Y. Shi, D. Fan, T. Ji, C. J. Yang, *Anal. Chem.* **2015**, *87*, 4941.
[157] H.-Y. Cao, A.-H. Yuan, W. Chen, X.-S. Shi, Y. Miao, *BMC Cancer* **2014**, *14*, 699.
[158] M. Liu, T. Yang, Z. Chen, Z. Wang, N. He, *Biomater. Sci.* **2018**, *6*, 3152.
[159] X. Zhang, J. Zhang, Y. Ma, X. Pei, Q. Liu, B. Lu, L. Jin, J. Wang, J. Liu, *Int. J. Biochem. Cell B.***2014**, *46*, 1.
[160] X. Li, W. Zhang, L. Liu, Z. Zhu, G. Ouyang, Y. An, C. Zhao, C. J. Yang, *Anal. Chem.* **2014**, *86*, 6596.
[161] C.-Y. Wang, B.-L. Lin, C.-H. Chen, *Int. J. Cancer* **2016**, *138*, 918.
[162] J. He, J. Wang, N. Zhang, L. Shen, L. Wang, X. Xiao, Y. Wang, T. Bing, X. Liu, S. Li, et al., *Talanta* **2019**, *194*, 437.
[163] Z.-X. Huang, Q. Xie, Q.-P. Guo, K.-M. Wang, X.-X. Meng, B.-Y. Yuan, J. Wan, Y.-Y. Chen, *Chinese Chem. Lett.* **2017**, *28*, 1252.
[164] X. Wu, H. Liang, Y. Tan, C. Yuan, S. Li, X. Li, G. Li, Y. Shi, X. Zhang, *PLoS ONE* **2014**, *9*, e90752.
[165] B. Yuan, X. Jiang, Y. Chen, Q. Guo, K. Wang, X. Meng, Z. Huang, X. Wen, *Talanta* **2017**, *170*, 56.
[166] Y. An, Y. Hu, X. Li, Z. Li, J. Duan, X.-D. Yang, *Sci Rep* **2019**, *9*, 7343.
[167] Z. Liu, J.-H. Duan, Y.-M. Song, J. Ma, F.-D. Wang, X. Lu, X.-D. Yang, *J Transl Med* **2012**, *10*, 148.
[168] D. Shangguan, Z. Cao, L. Meng, P. Mallikaratchy, K. Sefah, H. Wang, Y. Li, W. Tan, *J. Proteome Res.* **2008**, *7*, 2133.
[169] A. T. Bayrac, K. Sefah, P. Parekh, C. Bayrac, B. Gulbakan, H. A. Oktem, W. Tan, *ACS Chem. Neurosci.* **2011**, *2*, 175.

[170] S. Camorani, C. L. Esposito, A. Rienzo, S. Catuogno, M. Iaboni, G. Condorelli, V. de Franciscis, L. Cerchia, *Mol. Ther.* **2014**, *22*, 828.
[171] P. J. Bates, D. A. Laber, D. M. Miller, S. D. Thomas, J. O. Trent, *Exp. Mol. Pathol.* **2009**, *86*, 151.
[172] P. J. Bates, E. M. Reyes-Reyes, M. T. Malik, E. M. Murphy, M. G. O'Toole, J. O. Trent, *BBA-Gen. Subjects* **2017**, *1861*, 1414.
[173] J. E. Rosenberg, R. M. Bambury, E. M. Van Allen, H. A. Drabkin, P. N. Lara, A. L. Harzstark, N. Wagle, R. A. Figlin, G. W. Smith, L. A. Garraway, et al., *Invest New Drugs* **2014**, *32*, 178.
[174] P. Charoenphol, H. Bermudez, *Mol. Pharmaceutics* **2014**, *11*, 1721.
[175] Q. Li, D. Zhao, X. Shao, S. Lin, X. Xie, M. Liu, W. Ma, S. Shi, Y. Lin, *ACS Appl. Mater. Interfaces* **2017**, *9*, 36695.
[176] S. M. Taghdisi, N. M. Danesh, M. Ramezani, R. Yazdian-Robati, K. Abnous, *Mol. Pharmaceutics* **2018**, *15*, 1972.
[177] S. Li, Q. Jiang, S. Liu, Y. Zhang, Y. Tian, C. Song, J. Wang, Y. Zou, G. J. Anderson, J.-Y. Han, et al., *Nat Biotechnol* **2018**, *36*, 258.
[178] S. M. Douglas, I. Bachelet, G. M. Church, *Science* **2012**, *335*, 831.
[179] G. Zhu, J. Zheng, E. Song, M. Donovan, K. Zhang, C. Liu, W. Tan, *P. Natl. Acad. Sci.* **2013**, *110*, 7998.
[180] I. Monaco, S. Camorani, D. Colecchia, E. Locatelli, P. Calandro, A. Oudin, S. Niclou, C. Arra, M. Chiariello, L. Cerchia, et al., *J. Med. Chem.* **2017**, *60*, 4510.
[181] S. Shi, W. Fu, S. Lin, T. Tian, S. Li, X. Shao, Y. Zhang, T. Zhang, Z. Tang, Y. Zhou, et al., *Nanomedicine* **2019**, *21*, 102061.
[182] F. Wang, Y. Zhou, S. Cheng, J. Lou, X. Zhang, Q. He, N. Huang, Y. Cheng, *Nanoscale Res Lett* **2020**, *15*, 150.
[183] I. A. P. Thompson, L. Zheng, M. Eisenstein, H. T. Soh, *Nat Commun* **2020**, *11*, 2946.
[184] W. Fu, L. Tang, G. Wei, L. Fang, J. Zeng, R. Zhan, X. Liu, H. Zuo, C. Z. Huang, C. Mao, *Angew. Chem. Int. Ed.* **2019**, *58*, 16405.
[185] J. A. Lee, M. C. DeRosa, *Chem. Commun.* **2010**, *46*, 418.
[186] Y. Boulard, J. A. H. Cognet, J. Gabarro-Arpa, M. Le Bret, L. C. Sowers, G. V. Fazakerley, *Nucleic Acids Res.* **1992**, *20*, 1933.
[187] P. Sun, N. Zhang, Y. Tang, Y. Yang, X. Chu, Y. Zhao, *IJN* **2017**, *12*, 2657.
[188] Z. Ge, L. Guo, G. Wu, J. Li, Y. Sun, Y. Hou, J. Shi, S. Song, L. Wang, C. Fan, et al., *Small* **2020**, *16*, 1904857.
[189] G. Zhang, Z. Zhang, J. Yang, *Nanoscale Res Lett* **2017**, *12*, 495.
[190] H. Lee, A. K. R. Lytton-Jean, Y. Chen, K. T. Love, A. I. Park, E. D. Karagiannis, A. Sehgal, W. Querbes, C. S. Zurenko, M. Jayaraman, et al., *Nature Nanotech* **2012**, *7*, 389.
[191] D. H. Schaffert, A. H. Okholm, R. S. Sørensen, J. S. Nielsen, T. Tørring, C. B. Rosen, A. L. B. Kodal, M. R. Mortensen, K. V. Gothelf, J. Kjems, *Small* **2016**, *12*, 2634.
[192] J. Yan, J. Chen, N. Zhang, Y. Yang, W. Zhu, L. Li, B. He, *J. Mater. Chem. B* **2020**, *8*, 492.
[193] C. Tao, Y. J. Chuah, C. Xu, D.-A. Wang, *J. Mater. Chem. B* **2019**, *7*, 357.
[194] D. A. Yardley, *J. Control. Release* **2013**, *170*, 365.
[195] R. Kinoshita, Y. Ishima, V. T. G. Chuang, H. Nakamura, J. Fang, H. Watanabe, T. Shimizu, K. Okuhira, T. Ishida, H. Maeda, et al., *Biomaterials* **2017**, *140*, 162.
[196] J. Mikkilä, A.-P. Eskelinen, E. H. Niemelä, V. Linko, M. J. Frilander, P. Törmä, M. A. Kostiainen, *Nano Lett.* **2014**, *14*, 2196.
[197] S. D. Perrault, W. M. Shih, *ACS Nano* **2014**, *8*, 5132.
[198] N. F. Steinmetz, S. Lim, F. Sainsbury, *Biomater. Sci.* **2020**, *8*, 2771.

[199] P. Nédellec, P. Vicart, C. Laurent-Winter, C. Martinat, M.-C. Prévost, M. Brahic, *J. Virol.* **1998**, *72*, 9553.
[200] K. J. Koudelka, G. Destito, E. M. Plummer, S. A. Trauger, G. Siuzdak, M. Manchester, *PLoS Pathog* **2009**, *5*, e1000417.
[201] H. Hu, H. Masarapu, Y. Gu, Y. Zhang, X. Yu, N. F. Steinmetz, *ACS Appl. Mater. Interfaces* **2019**, *11*, 18213.
[202] C.-W. Huang, Z. Li, P. S. Conti, *J. Nucl. Med.* **2011**, *52*, 1979.
[203] F. Fontana, D. Liu, J. Hirvonen, H. A. Santos, *WIRES Nanomed. Nanobi.* **2017**, *9*, e1421.
[204] H. Gonzalez, C. Hagerling, Z. Werb, *Genes Dev.* **2018**, *32*, 1267.
[205] H. H. van Ojik, L. Bevaart, C. E. Dahle, A. Bakker, M. J. H. Jansen, M. J. van Vugt, J. G. J. van de Winkel, G. J. Weiner, *Cancer Res* **2003**, *63*, 5595.
[206] D. M. Klinman, *Nat Rev Immunol* **2004**, *4*, 249.
[207] C. Martínez-Campos, A. I. Burguete-García, V. Madrid-Marina, *Viral Immunol.* **2017**, *30*, 98.
[208] S. Lee, K. Margolin, *Cancers* **2011**, *3*, 3856.
[209] G. Yang, J. E. Koo, H. E. Lee, S. W. Shin, S. H. Um, J. Y. Lee, *Biomed. Pharmacother.* **2019**, *112*, 108657.
[210] J. Li, H. Pei, B. Zhu, L. Liang, M. Wei, Y. He, N. Chen, D. Li, Q. Huang, C. Fan, *ACS Nano* **2011**, *5*, 8783.
[211] Y. Araie, Y. Takahashi, Y. Takahashi, Y. Takakura, M. Nishikawa, *Biol. Pharm. Bull.* **2018**, *41*, 564.
[212] H. Kaur, J. G. Bruno, A. Kumar, T. K. Sharma, *Theranostics* **2018**, *8*, 4016.
[213] Z. Fu, J. Xiang, *IJMS* **2020**, *21*, 2793.
[214] C.-W. Huang, Z. Li, P. S. Conti, *J. Nucl. Med.* **2011**, *52*, 1979.
[215] E. C. Costa, A. F. Moreira, D. de Melo-Diogo, V. M. Gaspar, M. P. Carvalho, I. J. Correia, *Biotechnol. Adv.* **2016**, *34*, 1427.
[216] B.-W. Huang, J.-Q. Gao, *J. Control. Release* **2018**, *270*, 246.

ToC

Delivery systems with stimuli-responsiveness not only provide precise control over the release of the cargo but they may also perform a predefined biomedical function which may further lead to better clinical outcome. This review focuses on DNA nanostructure-based stimuli-responsive therapies and nanometer-precise frameworks for future cancer therapeutics.

Iris Seitz, Ahmed Shaukat, Kurt Nurmi, Heini Ijäs, Jouni Hirvonen, Hélder A. Santos, Mauri A. Kostiainen,* and Veikko Linko*

Prospective Cancer Therapies Using Stimuli-Responsive DNA Nanostructures